Global Change Biology

Global Change Biology (2015) **21**, 3246–3266, doi: 10.1111/gcb.12951

INVITED REVIEW

Quantifying surface albedo and other direct biogeophysical climate forcings of forestry activities

RYAN M. BRIGHT[1,2], KAIGUANG ZHAO[3], ROBERT B. JACKSON[4] and FRANCESCO CHERUBINI[2]

[1]*Norwegian Forest and Landscape Institute, Ås, Norway,* [2]*Industrial Ecology Program, Energy and Process Engineering, Norwegian University of Science and Technology, Trondheim, Norway,* [3]*School of Environment and Natural Resources, Ohio Agricultural Research and Development Center, The Ohio State University, Wooster, OH, USA,* [4]*School of Earth Sciences, Woods Institute for the Environment and Precourt Institute for Energy, Stanford University, Palo Alto, CA, USA*

Abstract

By altering fluxes of heat, momentum, and moisture exchanges between the land surface and atmosphere, forestry and other land-use activities affect climate. Although long recognized scientifically as being important, these so-called biogeophysical forcings are rarely included in climate policies for forestry and other land management projects due to the many challenges associated with their quantification. Here, we review the scientific literature in the fields of atmospheric science and terrestrial ecology in light of three main objectives: (i) to elucidate the challenges associated with quantifying biogeophysical climate forcings connected to land use and land management, with a focus on the forestry sector; (ii) to identify and describe scientific approaches and/or metrics facilitating the quantification and interpretation of direct biogeophysical climate forcings; and (iii) to identify and recommend research priorities that can help overcome the challenges of their attribution to specific land-use activities, bridging the knowledge gap between the climate modeling, forest ecology, and resource management communities. We find that ignoring surface biogeophysics may mislead climate mitigation policies, yet existing metrics are unlikely to be sufficient. Successful metrics ought to (i) include both radiative and nonradiative climate forcings; (ii) reconcile disparities between biogeophysical and biogeochemical forcings, and (iii) acknowledge trade-offs between global and local climate benefits. We call for more coordinated research among terrestrial ecologists, resource managers, and coupled climate modelers to harmonize datasets, refine analytical techniques, and corroborate and validate metrics that are more amenable to analyses at the scale of an individual site or region.

Keywords: biophysical, climate impact, climate metric, forest management, land management, land-use change, review

Received 27 January 2015 and accepted 17 March 2015

Introduction

The terrestrial biosphere and Earth's climate are closely entwined. Climate strongly influences terrestrial productivity and biome distributions. In turn, the vegetation, soils, and other components of the terrestrial biosphere influence climate through the amount of energy, water, carbon, and other chemical species that they store and exchange with the atmosphere. Human interventions directly alter vegetation cover and structure through the conversion of one land-use type to another (i.e., forest to cropland), or through a change in management for an existing land-use type (e.g., conversion of hardwood to softwood forest; addition of irrigation or fertilization; extension of rotation length). In turn, such changes alter not just the carbon balance of a system but perturb surface solar and thermal infrared radiation budgets and atmospheric turbulence, leading to alterations in the fluxes of heat, water vapor, momentum, CO_2, other trace gases, and organic and inorganic aerosols between the land surface and the atmosphere (Pielke *et al.*, 1998; 2011). A deeper quantitative understanding of how human intervention on land will affect climate regulation – and over which temporal and spatial scales – is essential for successful climate change mitigation (Feddema *et al.*, 2005; Jackson *et al.*, 2008; Mahmood *et al.*, 2010).

Historically, extensive land cover or management changes (LCC or LMC) have entailed forest conversions to crops or grasslands for agriculture (Goldewijk, 2001; Pongratz *et al.*, 2008). Although the pace of global deforestation has slowed in recent decades (Meyfroidt *et al.*, 2010, FAO & JRC, 2012), the integrated assessment modeling (IAM) community (Van Vuuren *et al.*, 2011) and the 5th Assessment Reports of the IPCC suggest that forests will play an increasingly large role in climate change mitigation and adaptation (Smith *et al.*, 2014; Settele *et al.*, 2014) – whether land areas are re-/

Correspondence: Ryan M. Bright, e-mail: rbr@skogoglandskap.no

© 2015 John Wiley & Sons Ltd

afforested or whether existing forests are managed more intensively.

Relative to our understanding of forests' role in the global carbon cycle, our understanding of their non-CO_2 influences on atmospheric chemistry and climate is in its infancy. Apart from providing carbon sequestration services, forest ecosystems emit biogenic volatile organic compounds (BVOCs) that can rapidly oxidize in the atmosphere, generating O_3 and secondary organic aerosols (SOAs) (Arneth *et al.*, 2010). This biogeochemical mechanism impacts climate both directly and indirectly (Spracklen *et al.*, 2008; Scott *et al.*, 2014), and its global magnitude has only recently been examined (Unger, 2014).

However, more established scientifically are forests' direct biogeophysical contributions to the climate system: that is, their regulation of the exchanges of energy, water, and momentum between the earth's surface and lower atmosphere (Fig. 1). Within the climate science and global change research communities, forest cover and management changes, and the corresponding changes in surface biophysics are increasingly recognized as important forcings of local, regional, and global climate (Zheng *et al.*, 2002; Durieux *et al.*, 2003; Mohr *et al.*, 2003; Avissar & Werth, 2005; Ray *et al.*, 2006; Betts *et al.*, 2007a; Juang *et al.*, 2007; Abiodun *et al.*, 2008; Klingaman *et al.*, 2008; Montenegro *et al.*, 2009; Lohila *et al.*, 2010; Rotenberg & Yakir, 2010, 2011; Arora & Montenegro, 2011; Kirschbaum *et al.*, 2011; Lee *et al.*, 2011; Swann *et al.*, 2011; Chen *et al.*, 2012; Lawrence *et al.*, 2012; Rogers *et al.*, 2013; Peng *et al.*, 2014; Wang *et al.*, 2014; Zhang *et al.*, 2014; Zhao & Jackson, 2014; Schwaab *et al.*, 2015). Outside these communities, however, biogeophysical climate impacts from LCC and LMC are rarely quantified or even acknowledged, with forest sector policies typically based strictly on carbon cycle dimensions. Most climate assessments overlook forest biogeophysical effects altogether due to the many complexities and challenges involved in quantifying them (Pielke *et al.*, 2002).

Our aim here is therefore to shed light on some of these complexities and the challenges of measuring and quantifying biogeophysical climate impacts connected to LCC and LMC, with a predominant focus on forestry (henceforth FCC and FMC). To that end, we review the scientific literature, relying as much as possible on observation-based studies while recognizing modeling studies that have made important contributions. Previous reviews have focused more generally on the full suite of biogeophysical impacts of land-use and land cover changes on climate (Pielke *et al.*, 1998, 2007, 2011; Pielke, 2001; Foley *et al.*, 2003; Mahmood *et al.*, 2013; Devaraju *et al.*, 2015), although some have taken a narrower focus on forested ecosystems (Bonan, 2008; Jackson *et al.*, 2008; Anderson *et al.*, 2010) or on LCC/LMC metrics suitable for use in specific analytical frameworks (Bright, 2015a). Here, we focus our review on the fundamental physical mechanisms by which forested ecosystems directly affect climate and on quantitative assessment methods and/or metrics relevant to forest management decision making.

Our review is structured as follows: We first present surface energy and moisture budgets and describe how they are modulated by both biological and environmental controls. We then elaborate in greater detail the types of information that are needed to quantify the individual fluxes of the surface energy balance, including albedo, followed by an illustration of how these fluxes may be used to compute various climate metrics. We then present two case studies and apply and compare the various metrics, demonstrating the importance of key assumptions and methodological considerations differentiating them. We then conclude with a discussion on the relevancy of the presented climate metrics and identify areas of critical research needs.

Mechanisms

Surface energy and moisture budgets

FCC/FMC affects climate by altering surface moisture and energy budgets, which can be written as:

$$R_{\mathrm{SW}}^{\downarrow}(1-\alpha_s)+R_{\mathrm{LW}}^{\downarrow}-R_{\mathrm{LW}}^{\uparrow}=R_N=R_G+H+L(E+T) \tag{1}$$

$$P=\mathrm{RO}+I+E+T \tag{2}$$

where Eqn (1) is the surface energy budget and Eqn (2) is the surface moisture budget, with their individual terms defined in Table 1. They are presented together because they are intimately linked (Pielke, 2001). For instance, the latent heat flux $L(E+T)$is directly related to the amount of moisture exchanged from the surface to the atmosphere $(E+T)$ which is governed largely by moisture availability $(P-\mathrm{RO}-I)$ (Wang & Dickinson, 2012). For example, owed to their deeper rooting depths and enhanced ability to access water stored in soils, $L(E+T)$ fluxes in temperate forests can remain relatively high compared to grasslands during times of drought, when $L(E+T)$ fluxes would otherwise be similar to forests under wet conditions (Stoy *et al.*, 2006). Thus, a change to any term in Eqn (1) or (2) will affect the heat and moisture fluxes within the planetary boundary layer and potentially affect

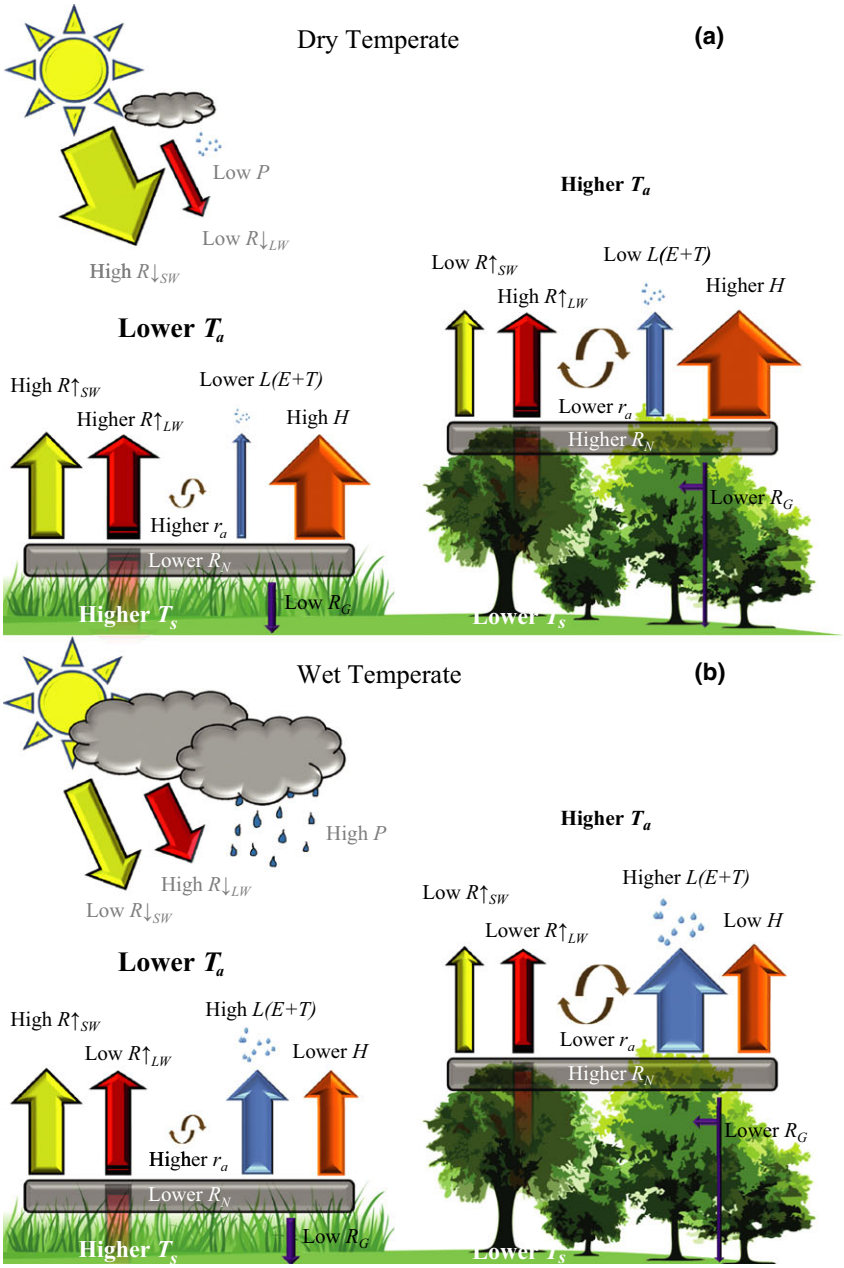

Fig. 1 Differences in the annual surface energy and moisture budgets between a temperate forest and an open grassland under dry (a) and wet (b) conditions. Horizontal fluxes of heat and moisture are excluded, and 'R_G' includes heat stored by both the ground and vegetation. Although annual 'R_N' is partitioned differently under arid and wet conditions, annual sensible heat fluxes ('H') in temperate forests are typically higher relative to the grassland. 'T_a' = air temperature; 'r_a' = aerodynamic resistance.

atmospheric water vapor, cloud formation, precipitation, and atmospheric circulation patterns. These boundary layer processes are dynamic, variable, and difficult to predict, which generally limits the ability to predict the impact of land-use change and landscape dynamics on climate patterns (Cotton & Pielke, 1995; Pielke, 2001). Quantifying the full climate change effect of forest cover or management changes at (inter)annual timescales is thus unrealistic for site-level observations. Such an approach requires coupled surface–atmosphere models to account for boundary layer dynamics, atmospheric albedo from clouds, and frontal and convective precipitation (Mahmood *et al.*, 2013; Devaraju *et al.*, 2015).

However, an analysis of changes in the major components of the surface energy and moisture budgets due

Table 1 Nomenclature. Variable 'type' denotes how the variables are used in surface energy and moisture budget paramaterizations throughout the review

Variable notation	Unit	Definition	Type of variable	Function of:
LAI	$m^2\ m^{-2}$	Leaf Area Index	Structural	
LAI_e	$m^2\ m^{-2}$	Effective LAI	Structural	LAI
SAI	$m^2\ m^{-2}$	Stem Area Index	Structural	
h_c	m	Canopy height	Structural	
f_{cs}	%	Fraction of canopy intercepted snow	Structural & Environmental	SAI; LAI; T_a; P
f_g	%	Ground fraction	Structural	LAI
α_{g0}	Unitless	Snow-free ground albedo	Physiological & Environmental	α_{leaf}; α_{soil}; τ_{leaf}
f_{gs}	%	Fraction of ground covered snow	Structural & Environmental	LAI; T_a; P
α_{sn}	Unitless	Snow albedo	Environmental	P; T_a
α_{c0}	Unitless	Snow-free canopy albedo	Physiological & Environmental	α_{leaf}; α_{branch}
P	mm	Precipitation	Moisture budget term	
RO	mm	Runoff	Moisture budget term	
I	mm	Infiltration	Moisture budget term	
T_a	°C	Air temperature	Environmental	H; $L(E\&T)$
T_s	°C	Surface temperature	Surface energy budget term	λ; R_N
λ	$°C(Wm^{-2})^{-1}$	Temperature sensitivity	Environmental	
$R^{\uparrow}_{LW}$	Wm^{-2}	Outgoing longwave radiation emitted at surface	Surface energy budget term	T_s; ε_s; σ
σ	$Wm^{-2°C\ -4}$	Stefan–Boltzmann constant	Constant	
s	kPa $°C^{-1}$	Slope of saturation vapor pressure–temperature curve	Environmental	T_a; RH
VPD	kPa	Vapor pressure deficit	Environmental	T_a; RH
AP	kPa	Air pressure	Environmental	
RH	%	Relative humidity	Environmental	e_w; e^*_w
ρ	kgm^{-3}	Air density	Environmental	
γ	kPa $°C^{-1}$	Psychrometric constant	Environmental	
ε_s	Unitless	Surface emissivity	Surface energy budget term	
α_s	Unitless	Surface albedo	Surface energy budget term	f_g; α_{g0}; f_{gs}; α_{sn}; α_{c0}
C_s	$Jm^{-3}°C^{-1}$	Soil volumetric heat capacity	Environmental	
C_p	$Jm^{-3}°C^{-1}$	Air volumetric heat capacity	Environmental	
k_s	$Wm^{-1}°C^{-1}$	Soil thermal conductivity	Environmental	
$R^{\downarrow}_{LW}$	Wm^{-2}	Incoming longwave radiation at surface level	Surface energy budget term	RH; $R^{\downarrow}_{SW}/R^{\downarrow}_{SW,clear}$
R_G	Wm^{-2}	Ground heat storage from conduction	Surface energy budget term	LAI; C_s; k_s
$L(E+T)$	Wm^{-2}	Latent heat flux from evaporation & transpiration	Surface energy budget term	r_a; r_c; C_p; ρ; VPD; s; γ; $(R_N - R_G)$
L	$MJkg^{-1}$	Latent heat of vaporization	Environmental	T_a
E	mm	Evaporation	Environmental	r_a; C_p; ρ; VPD; s; γ; $(R_N - R_G)$
T	mm	Transpiration	Physiological; Environmental	r_a; r_c; C_p; ρ; VPD; s; γ; $(R_N - R_G)$
H	Wm^{-2}	Sensible heat flux	Surface energy budget term	r_a; C_p; ρ; T_s-T_a
u	ms^{-1}	Wind speed	Environmental	
d	m	Zero plane displacement height	Structural	LAI; h_c
z_0	m	Momentum roughness length	Structural	LAI; h_c
$R^{\downarrow}_{SW}$	Wm^{-2}	Incoming shortwave radiation incident at surface (insolation)	Surface energy budget term	
R_N	Wm^{-2}	Net radiation	Surface energy budget term	

Table 1 (continued)

Variable notation	Unit	Definition	Type of variable	Function of:
				$R_{SW}^{\downarrow}$; α_s; $R_{LW}^{\downarrow}$; σ; ε_s; T_s
β	Unitless	Bowen ratio	Surface energy budget term	H; $L(E + T)$
g_a (r_a)	$m^2s^{-1}(sm^{-2})$	Bulk aerodynamic conductance (resistance)	Structural & Environmental	LAI; h_c; u
g_c (r_c)	$m^2s^{-1}(sm^{-2})$	Bulk canopy or surface conductance (resistance)	Structural & Physiological	LAI_e; g_l
g_s (r_s)	$m^2s^{-1}(sm^{-2})$	Leaf stomatal conductance (resistance)	Physiological	
z_r	m	Rooting depth	Physiological	
RF_{SW}^{TOA}	Wm^{-2}	Shortwave radiative forcing at top-of-atmosphere (TOA)	LCC/LMC climate metric	$\Delta\alpha_s$
$T_{SW}^{\uparrow}$	Unitless	Share of reflected SW radiation at surface arriving at TOA	Environmental	
LCC		Land cover change		
LMC		Land management change		
FCC		Forest cover change		
FMC		Forest management change		

to FCC/FMC can contribute to an understanding of first-order biogeophysical effects. Changes in Eqn (1) will result in a change in the land surface temperature, as the radiation that impinges on the surface must be balanced by the reflected and emitted radiation and by energy lost or gained through H, $L(E + T)$, and R_G. Air temperatures can also be affected by a change in H and $L(E + T)$, with a magnitude that depends on the depth of the atmospheric boundary layer (Baldocchi & Ma, 2013). Vegetation cover change that results in a long-term perturbation in air temperature can potentially affect ecosystem structure and functioning (Mcguire *et al.*, 2006; Chapin *et al.*, 2012). For example, a switch in vegetation could create warmer surface conditions and enhance rates of soil respiration, potentially decreasing net ecosystem productivity through enhanced soil respiration in the short term (Rustad *et al.*, 2001). It is therefore important to quantify vegetation feedbacks on local climate and to attribute this to FMC/FMC. This necessitates a deeper understanding of the relative roles of structural, physiological, and environmental controls on surface energy and moisture budgets, and a need to quantify these with meaningful metrics.

Vegetation structure

Structural parameters such as leaf area index (LAI) and vegetation height play an important role in determining resistances (or conductivities) to heat, moisture, and momentum transfer. When a parcel of turbulent air meets a vegetated stand, wind speed is reduced, transferring momentum from the atmosphere to the surface, creating turbulence that mixes the air and transports heat and water from the surface into the lower atmosphere (Bonan, 2002; Oke, 2002; Monteith & Unsworth, 2008). The transport of momentum, heat, and moisture is more efficient with greater height above the surface and with densely vegetated canopies. LAI and forest canopy heights thus play an essential role in determining roughness lengths and aerodynamic resistances to heat, moisture, and momentum between the canopy and atmospheric. Relative to shorter statured vegetation such as croplands and grasslands, forested surfaces have higher roughness lengths and lower aerodynamic resistances that facilitate more sensible heat and water vapor dissipation away from the surface during the daytime (Hoffmann & Jackson, 2000).

Together with stem area index (SAI), LAI is also an important structural variable determining the surface albedo and hence net radiation R_N. SAI and LAI control the amount of solar radiation incident at the ground level which is often covered in snow during winter in many temperate and boreal regions. The albedo of snow is much higher than the albedo of foliage or branches, thus SAI and LAI play central roles in regulating radiation budgets in regions with significant snow cover by contributing to the 'masking' of the underlying snow surface and hence the total albedo. Across North America between 45 and 60°N, the zonally averaged white-sky albedo in January was at least twice as high for croplands and grasslands (0.57 and 0.50, respectively) compared to locations with

deciduous broadleaf or evergreen needleleaf forests (0.26 and 0.20, respectively (Zhao & Jackson, 2014).

LAI is also an important variable determining bulk canopy conductance to heat and moisture transfer, thus acting as controls on T as well as intercepted precipitation and canopy E. In nonarid regions, in summer, E & T are often highly correlated with LAI (see Wang & Dickinson (2012) and cited studies therein).

Vegetation physiology

Tree physiology plays an important role in governing T and I. For example, stomatal conductance (inverse of resistance) directly control rates of T at the individual leaf level, while root structure and depth affect T through access to soil water. Root structure and depth also affect I and the water storage capacity of soils (and thereby indirectly that which is ultimately available for T and soil E). Forest management decisions that lead to a change in tree species directly affect physiological controls of surface energy and moisture budgets. For example, under nondrought conditions and given equal LAIs, a shift toward more loblolly pine plantation area (*Pinus taeda* L.) at the expense of oak–hickory hardwood area (*Quercus – Carya*) would increase regional T [and $L(T)$] in the SE USA due to the loblolly pine's higher leaf stomatal conductance (Stoy *et al.*, 2006).

Environmental controls and feedbacks with the energy balance

Local meteorological conditions can play an equally large role in determining surface energy and moisture budgets. For instance, R_N is determined by $R_{SW}^{\downarrow}$ which is affected by cloud cover and by surface albedo α_s, which can be affected by temperature and P (snow has a higher albedo than dry soil which has a higher albedo than wet soil). The partitioning of the turbulent heat fluxes ($R_N - R_G$) into H and $L(E + T)$ is also partially controlled by differences between the air and surface temperatures and by differences in saturated vs. actual vapor pressures (i.e., the vapor pressure deficit), with vapor pressure having an exponential relationship with air temperature (Bonan, 2002; Monteith & Unsworth, 2008). Wind speed also determines the aerodynamic resistance of the surface–atmospheric boundary layer, with resistance decreasing as wind speeds increase.

Table 2 describes the individual variables in Eqn (1) in terms of their important controls. Refer to Table 1 for variable definitions.

Quantifying surface energy fluxes

Radiative energy exposed to vegetation is partitioned and transferred to the atmosphere by convection and evaporation of water, with consequent impacts on the surface radiative temperature, T_s. Convective heat transfer of sensible heat H is directly proportional to the difference in air temperature at some reference height and at the surface level and is inversely related to an overall aerodynamic resistance r_a:

$$H = \rho C_p (T_a - T_s)/r_a \tag{3}$$

where ρ is the air density (kg m^{-3}), C_p is the heat capacity of air (J kg^{-1} °C^{-1}), and r_a is the overall aerodynamic resistance to heat transfer from the surface to the atmospheric boundary layer.

The transfer of latent heat ($L(E + T)$) is directly proportional to the difference in the vapor pressure of air at some reference height and at the surface level and is also inversely related to an overall resistance. Latent heat exchanges can be parameterized in a variety of ways, although the Penman–Monteith equation (Monteith, 1965) is widely considered an accurate expression to estimate $E + T$ (Allen *et al.*, 1989, 1998),

Table 2 Surface energy budget variables [Eqn (1)] and their controls

			Controls		
Variable notation	Unit	Definition	Environmental	Structural	Physiological
α_s	Unitless	Surface albedo, $R_{SW}^{\uparrow} R_{SW}^{\downarrow -1}$	α_{sn}; P; T_a	LAI; SAI	α_{leaf}; τ_{leaf}
$R_{SW}^{\downarrow}$	Wm^{-2}	Incoming solar radiation at surface	τ_{atm}; α_{atm}; latitude		
$R_{LW}^{\downarrow}$	Wm^{-2}	Incoming longwave radiation incident at surface	τ_{atm}; α_{atm}; ε_{atm}; T_a; RH		
R_G	Wm^{-2}	Heat storage flux from conduction	k_s; C_s	LAI; SAI	
H	Wm^{-2}	Turbulent sensible heat flux	C_p; ρ; u; $T_s - T_a$	h_c; LAI (in z_0, in r_a)	
$L(E + T)$	Wm^{-2}	Turbulent latent heat flux	VPD, C_p; ρ; T_a; u; s; γ	LAI_e (in r_c)	r_s, z_r
ε_s	Unitless	Surface emissivity			
$R_{LW}^{\uparrow}$	Wm^{-2}	Outgoing longwave radiation emitted by the surface	T_s; ε_s		

developed to use surface radiation, temperature, and humidity data (Wang & Dickinson, 2012). For forests, the surface can be regarded as a 'big leaf' (Deardorf 1978) in which a separate resistance to water vapor transfer from the canopy is introduced:

$$L(E+T) = \frac{s(R_N - R_G) + \rho C_p \mathrm{VPD}/r_a}{s + (1 + r_c/r_a)\gamma} \quad (4)$$

where s is the slope of the saturation vapor pressure–temperature curve (kPa °C^{-1}) (Tetens, 1930; Murry, 1967), VPD is the vapor pressure deficit (kPa; a function of T_a and relative humidity), γ is the psychrometric constant (kPa °C^{-1}), and r_c is the canopy resistance to water vapor transfer. Eqns (3) and (4) demonstrate that both the canopy and aerodynamic resistance terms are critical parameters controlling turbulent heat (and moisture) exchanges with the atmosphere, with the former being aerodynamically controlled and the latter being both aerodynamically and physiologically controlled.

Canopy resistance

At the scale of an individual leaf, stomatal control of transpiration is known as the leaf stomatal resistance r_l. At the scale of a canopy of leaves, canopy resistance r_c is used to describe the aggregate resistance. It is often calculated by scaling up the leaf stomatal resistance (r_s) of the leaves acting in parallel while treating the canopy as one 'big leaf':

$$r_c = \frac{r_l}{\mathrm{LAI}_e} \quad (5)$$

where LAI_e is the effective LAI which is empirically equal to the actual LAI for LAI ≤ 2, LAI/2 for LAI ≥ 4, and 2 for others (Ding *et al.*, 2014). 'Dual-leaf' canopy resistance models that take into account the share of sunlit vs. shaded leaves in the canopy often give more accurate results than the 'big leaf' model but require additional computations of the sunlit fraction and separate values of mean leaf stomatal resistances for shaded and unshaded leaves (Irmak *et al.*, 2008; Zhang *et al.*, 2011; Ding *et al.*, 2014). Typical r_s and r_c values for a range of vegetation types are presented in Table 3.

Canopy resistance is sometimes referred to as surface resistance when it describes the aggregate resistance of all transpiration and evaporation processes occurring on the ground and in the canopy including the evaporation of water intercepted by the canopy. The most advanced models for predicting *E & T* typically estimate separate surface resistances for *T*, *E* occurring at the ground level, and *E* occurring in the vegetation canopy (Wang & Dickinson, 2012).

Table 3 Typical minimum canopy (r_c) and leaf stomatal resistances (r_s) for various vegetation types [adapted from Kelliher *et al.* (1995)]. Effective LAI ('LAI_e') is deduced with Eqn (5)

Vegetation type	r_s (s m^{-1})	r_c (s m^{-1})	LAI_e
Temperate grassland	125	60	2.1
Coniferous forest	175	50	3.5
Temperature deciduous forest	215	50	4.3
Tropical rainforest	165	80	2.1
Cereal crops	90	30	3
Broadleaved herbaceous crops	80	35	2.3

Figure 2 illustrates the contribution to the daily latent heat flux from *T* and *E* occurring at the surface and in the canopy (from intercepted moisture) at neighboring sites in eastern Norway estimated with the Penman–Monteith scheme of Mu *et al.* (2011). The difference in total $L(E+T)$ between the two sites (sharing identical environmental controls) stems mostly from the additional contribution by *T* and canopy *E* at the mature forest site. The region is not moisture limited, thus the contribution from soil *E* is large at both sites and dominates total *E* + *T* throughout most of the year (Fig. 2, green).

Aerodynamic resistance

Sources of heat and water vapor will generally be found lower in the canopy than the apparent sink of momentum; thus; the overall aerodynamic resistances to heat and mass transfer may be described in terms of r_{am} – the aerodynamic resistance to momentum transfer, and r_b – an additional resistance term assumed to be identical for heat and water vapor (Monteith & Unsworth, 2008):

$$r_a = r_{\mathrm{am}} + r_b = \left[\log((z-d)/z_0)\right]^2/k^2u(z) + 2(ku_*)^{-1}\frac{\mathrm{Sc}^{0.67}}{\mathrm{Pr}} \quad (6)$$

where k is von Karman's constant (0.41), z is the reference height (m), d is the zero plane displacement height (m), $u(z)$ is the wind speed at reference height (m s^{-1}), z_0 is the roughness length of momentum (m), u_* is the friction velocity (around 0.05–0.1 u) (m s^{-1}), Sc is the Schmidt number, and Pr is the Prandtl number (the ratio of the two being the Lewis number or the ratio of thermal to mass diffusivity). The second right-hand expression in Eqn (6) is the additional resistance term (r_b) for rough or fibrous vegetation surfaces and is based on the empirical works of Thom (1972) and Wesely & Hicks (1977).

Key terms in Eqn (6) influencing the value of r_a are momentum roughness length z_0 and the zero plane

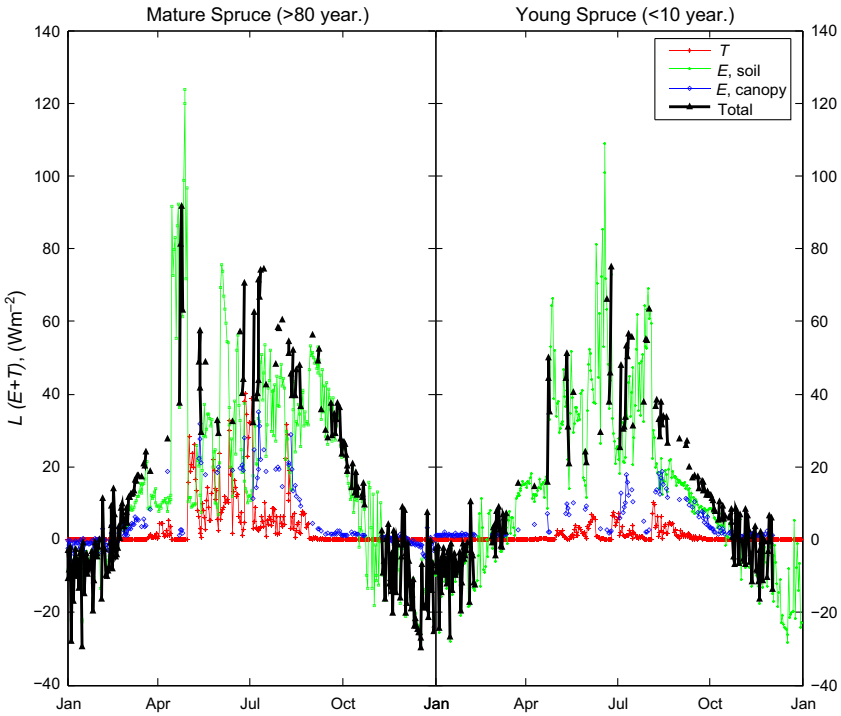

Fig. 2 Differences in the partitioning of daily E & T between adjacent young and mature spruce-dominant stands (*Picea abies* (L.) H. Karst.) in eastern Norway during 2006. Adapted from Bright *et al.* (2014).

displacement height d – both of which are often parameterized as a function of vegetation structure (Perrier, 1982; Pereira *et al.*, 1999):

$$d = h_c\left[1 - \frac{2}{\mathrm{LAI}}\left(1 - \mathrm{e}^{-\mathrm{LAI}/2}\right)\right] \tag{7}$$

$$z_0 = h_c \mathrm{e}^{-\mathrm{LAI}/2}(1 - \mathrm{e}^{-\mathrm{LAI}/2}) \tag{8}$$

where h_c is canopy height (m). Eqns (7) and (8) are valid for LAI ≥ 0.5 (Colaizzi *et al.*, 2004). Other empirical formulations can involve additional forest structural attributes such as stand density (number of trees per hectare) (Nakai *et al.*, 2008), but many modelers simply scale d with canopy height h_c [2/3 of h_c for forests and 1/8 of h_c for uniform crops (Allen *et al.*, 1998)].

What should be apparent when looking at Eqns (3)–(8) is that both canopy (or surface) and aerodynamic resistances are key terms controlling $L(E + T)$ and H, and these terms are in turn both largely determined by vegetation structure (i.e., LAI and h_c on d, z_0, and r_c) and physiology (i.e., r_l). While it is often assumed that decreases in $L(E + T)$ result in an increase in surface temperature, this is not always necessarily the case. T_s responds to changes in both aerodynamic roughness and the Bowen ratio – or the ratio of sensible to latent heat – which can be either positive or negative in response to FCC/FMC (Lee *et al.*, 2011).

Surface albedo

Surface albedo is one of the most important biogeophysical mechanisms acting on radiation budgets at both surface and top-of-atmosphere levels; hence, it affects both local and global climate (Otterman, 1977; Cess, 1978; Dickinson, 1983). Forests and taller vegetation are often darker than those with sparse or shorter vegetation (Henderson-Sellers & Wilson, 1983; Betts & Ball, 1997), particularly when the underlying surface is covered in snow or light-colored soil. In temperate and boreal regions, the interactions between forested vegetation and snow can significantly complicate the relationship between FCC/FMC and surface albedo changes (Pitman *et al.*, 2009; Boisier *et al.*, 2012; De Noblet-Ducoudré *et al.*, 2012; Bright *et al.*, 2015b).

Parameterizations of surface albedo (α_s) for forested areas differ with respect to their treatments of ground masking by vegetation and can be classified using three prevailing methods introduced in Qu & Hall (2007). Briefly, the first method estimates radiative transfer between the vegetation canopy and the ground surface; the second method combines the vegetation and ground albedos weighted by vegetation cover; and the third method combines the snow-free and snow albedo weighted by snow cover. Although no one particular approach is necessarily superior (Essery, 2013; Bright

et al., 2015b), we find it helpful to describe albedo using the second approach, where the surface albedo is a weighted share of the albedo of the ground and of the forest canopy (Verseghy *et al.*, 1993; Roesch & Roeckner, 2006):

$$\alpha_s = f_g\left[(1-f_{gs})\alpha_{g0} + f_{gs}\alpha_{sn}\right] + (1 - f_g)[(1-f_{cs})\alpha_{c0} + f_{cs}\alpha_{sn}] \quad (9)$$

where f_g is the fraction of exposed ground (sometimes referred to as the 'canopy gap fraction'), $1-f_g$ the fraction of the exposed canopy (sometimes referred to as the 'canopy radiative fraction'), f_{cs} the fraction of canopy covered with snow, f_{gs} the fraction of ground covered in snow, α_{sn} the albedo of snow, α_{g0} the snow-free ground albedo, and α_{c0} the snow-free canopy albedo. f_g (or 1-f_g) is determined by vegetation structure and is often a function of LAI and SAI. f_{cs} is often a function of canopy intercepted snow which is determined by both vegetation structure and local meteorology (Hedstrom & Pomeroy, 1998; Niu & Yang, 2004; Bartlett *et al.*, 2006; Essery *et al.*, 2009). α_{c0} is an intrinsic property of the vegetation largely determined by leaf level albedo and canopy structure (Sellers, 1985; Ollinger *et al.*, 2008; Hollinger *et al.*, 2010). $\alpha_{g0}$is largely determined by soil geology but varies with environmental factors influencing soil moisture (Idso *et al.*, 1975), whereas α_{sn} is purely controlled by environmental factors such as precipitation rates, wind, temperature, and other factors influencing snow grain size and impurities (such as soot deposition) (Wiscombe & Warren, 1980; Pirazzini, 2009).

FCC/FMC primarily affects α_s through alterations in vegetation structure and to some extent physiology. In addition to the surface energy budget, changes to α_s (henceforth $\Delta\alpha_s$) can directly alter the energy budget at the top-of-atmosphere (TOA) and hence global mean temperature (Bala *et al.*, 2007; Davin & De Noblet-Ducoudré, 2010; Arora & Montenegro, 2011).

Climate metrics

Radiative forcing

Shortwave radiative forcings (RFs) at the top of atmosphere (TOA) from albedo changes ($\Delta\alpha_s$) can be approximated with information on local insolation and atmospheric conditions:

$$\mathrm{RF}^{\mathrm{TOA}}_{\Delta\alpha_s} = R^{\downarrow}_{\mathrm{SW}}\Delta\alpha_s T^{\uparrow}_{\mathrm{SW}} \quad (10)$$

where $R^{\downarrow}_{\mathrm{SW}}$ is the local insolation ($\mathrm{Wm^{-2}}$), $\Delta\alpha_s$ is the local albedo change, and $T^{\uparrow}_{\mathrm{SW}}$ is the fraction of reflected $R^{\downarrow}_{\mathrm{SW}}$ arriving back at TOA. During multiple reflection and on the final trajectory of the reflected shortwave radiation toward TOA, there are opportunities for additional atmospheric absorption which reduces the impact of $\Delta\alpha_s$ upon the TOA flux change relative to its impact at the surface (Winton, 2005). This is accounted for in Eqn (10) through the use of an upward atmospheric transmittance parameter $T^{\uparrow}_{\mathrm{SW}}$. Locally, $T^{\uparrow}_{\mathrm{SW}}$ is difficult to measure/obtain, particularly if it is estimated using vertical profiles of optical properties, leading some to apply a value corresponding to the global annual mean, or 0.85 (Muñoz *et al.*, 2010; Cherubini *et al.*, 2012; Bright *et al.*, 2014; Caiazzo *et al.*, 2014), which was recently shown to be a reasonable assumption for use in site-specific analyses (Bright & Kvalevåg, 2013).

As an alternative to Eqn (10), one could apply 'radiative kernels' (Shell *et al.*, 2008; Soden *et al.*, 2008) that relate the change in TOA fluxes for a standard change in a surface property such as α_s. Global annual mean radiative kernels for $\Delta\alpha_s$ have been estimated to range between 1.29 and 1.61 ($\mathrm{W\ m^{-2}}$ $(0.01\Delta\alpha_s)^{-1}$) depending on the radiative transfer scheme and climate model (Shell *et al.*, 2008; Soden *et al.*, 2008).

Equation (10) represents a simple approximation of the local RF at TOA but does not account for variations of $R^{\downarrow}_{\mathrm{SW}}$ or $\Delta\alpha_s$ in time. Because $R^{\downarrow}_{\mathrm{SW}}$ and $\Delta\alpha_s$ covary in time, the most accurate quantifications of $\mathrm{RF}^{\mathrm{TOA}}_{\Delta\alpha_s}$ require high temporal resolution. This is especially critical in regions with seasonal snow cover, when surface albedos are higher yet when solar insolation is lower relative to snow-free months. Following conversion of forest to cropland (FCC), Bright (2015a) showed that estimates of the annual mean $\mathrm{RF}^{\mathrm{TOA}}_{\Delta\alpha_s}$ deviated as much as 62% when the annual $R^{\downarrow}_{\mathrm{SW}}$ and $\Delta\alpha_s$ values were used instead of the monthly values in its calculation.

In order to compute RF-based metrics or compare to other RF agents, the interannual RF of $\Delta\alpha_s$ is needed:

$$\mathrm{RF}^{\mathrm{TOA}}_{\Delta\alpha_s}(t,i) = \frac{\sum_{m=1}^{m=12} R^{\downarrow}_{\mathrm{SW}}(t,m,i)\Delta\alpha_s(t,m,i)T^{\uparrow}_{\mathrm{SW}}(t,m,i)\frac{A(t,m,i)}{A^{\mathrm{Earth}}}}{12} \quad [\mathrm{Wm^{-2}}] \quad (11)$$

where A is the local perturbed area, A_{Earth} is the area of the earth, m is the month, i is the location, and t is the analytical time step (1 year increments).

Global warming potential

In forestry and other land management projects, it can be useful to benchmark albedo change impacts

using a common currency such as CO_2-equivalents. Integrating $RF^{TOA}_{\Delta\alpha_s}(t,i)$ over time and normalizing to that of CO_2 provides the global warming potential of the albedo change impact in units of kg CO_2-eq. m^{-2}:

$$GWP_{\Delta\alpha_s}(TH,i) = \frac{\int_{t=0}^{TH} RF^{TOA}_{\Delta\alpha}(t,i)}{k_{CO_2}\int_{t=0}^{TH} y_{CO_2}(t)}\left[kgCO_2-eq.m^{-2}\right] \quad (12)$$

where TH is the integration or metric time horizon, k_{CO_2} is the radiative efficiency of a 1 kg increase of CO_2 in the atmosphere at a given concentration (Myhre *et al.*, 1998), and $y_{CO_2}(t)$ is the CO_2 impulse-response function – or the decay of anthropogenic CO_2 in the atmosphere over time following a 1 kg emission pulse (Joos *et al.*, 2013).

In rotation forestry, the albedo change following a clear-cut harvest can persist for several decades until the canopy of the new forest generation reaches closure. Unlike CO_2 in the atmosphere following an emission pulse in which the physical perturbation is long-lived, the albedo change is relatively short-lived (i.e., $\Delta\alpha_s(t) = 0$ when t = ~ 20–40 years for a typical boreal conifer); thus, the choice of TH is critical: higher THs minimize the contribution from albedo whereas lower THs give it stronger emphasis (revisited in the next section). Further, with time-integrated metrics like GWP, uncertainty increases with increasing TH, particularly for the predicted surface albedo change [$\Delta\alpha_s(t, i)$]; unlike the predicted change in atmospheric GHG concentration following an emission pulse, the albedo in the forest following FCC/FMC is subject to a higher risk of modification by humans or the environment (climate changes).

'Emissions equivalent from shortwave forcing' and 'Carbon drawdown equivalent'

Previous efforts to measure albedo changes from forestry projects in terms of their CO_2-equivalent effects (referred to as 'emission equivalent from shortwave forcing' or 'carbon drawdown equivalent') have been performed in the absence of information surrounding the lifetime and temporal dynamics of albedo changes following the change in forest cover (Betts, 2000; Zhao & Jackson, 2014). As a result, the lifetime and temporal dynamics of CO_2 in the atmosphere (i.e., $y_{CO_2}(t)$) are excluded from the CO_2-eq. characterization, which is overcome by use of CO_2's airborne fraction (AF) as a scaling factor. AF is the proportion of human-emitted CO_2 that remains in the atmosphere, which is typically around 0.45–0.5 and remains relatively constant over forestry timescales:

$$EESF_{\Delta\alpha_s}(i) = 2.72\frac{RF^{TOA}_{\Delta\alpha}(i)}{k_{CO_2}AF}\left[tC-eq.ha^{-2}\right] \quad (13)$$

where $RF^{TOA}_{\Delta\alpha}(i)$ is the instantaneous RF from an albedo change at location i and 2.72 is a scaling factor converting from kg CO_2-eq. m^{-2} to t C eq. ha^{-2} [the same scaling factor may also be applied to Eqn (12)].

Global mean temperature change

The extent to which $RF^{TOA}_{\Delta\alpha_s}$ impacts global mean surface temperatures can be estimated with application of a global climate sensitivity parameter λ that may describe either a transient or the equilibrium response by the global mean near-surface temperature to a unit $RF^{TOA}_{\Delta\alpha_s}$ (in $^{\circ}C(Wm^{-2})^{-1}$). The equilibrium temperature response can be expressed as a sum of two exponentials:

$$\delta T_a(t) = \sum_{i=1}^{2}\frac{c_i}{d_i}e^{\frac{-t}{d_i}} \quad (14)$$

where the sum of the coefficients c_i is the equilibrium climate sensitivity (λ) and d_i the two timescales due to the thermal inertial in Earth's ocean heat sinks (Ricke & Caldeira, 2014). For computing emission metrics, the IPCC 5th Assessment Report uses the following parameters, taken from (Boucher & Reddy, 2008): c_1 = 0.631 K/(Wm^{-2}), c_2 = 0.429 K/(Wm^{-2}), d_1 = 8.4 year, d_2 = 409.5 year.

The global mean surface temperature to a radiative forcing profile derived from a surface albedo change can be estimated through a convolution integral between the global $RF^{TOA}_{\Delta\alpha_s}$ and δT_a:

$$\Delta T_{\Delta\alpha_s}(t) = \int_0^t RF^{TOA}_{\Delta\alpha_s}(t)\delta T_a(t-t')dt' \quad (15)$$

where $RF^{TOA}_{\Delta\alpha_s}$ is the instantaneous albedo change RF and δT_a is the temperature-response function from above [Eqn (14)]. The use of the same climate sensitivity parameters for albedo and CO_2 radiative forcings implies that RFs from the two lead to the same global mean temperature response regardless of the location in which the physical perturbations originate – both vertically (surface vs. troposphere) and horizontally (globally distributed vs. confined to specific regions). The extent to which $RF^{TOA}_{\Delta\alpha_s}$ affects global mean surface temperature is highly uncertain and is discussed in greater detail in the final section.

Surface energy budget decomposition and local surface temperature changes

It is often useful to know the relative contribution of the radiative and nonradiative feedbacks directly influencing the local surface climate. Some researchers have formalized approaches to estimate a discrete change in the surface temperature by rearranging terms of the surface energy balance and taking first-order derivatives to assess radiative and nonradiative terms in isolation (Juang *et al.*, 2007; Lee *et al.*, 2011; Luyssaert *et al.*, 2014). Based on the findings of Juang *et al.* (2007) that heat storage (R_G) and emissivity (ε_s) terms of Eqn (1) are negligible on annual timescales, Lee *et al.* (2011) formulated an alternative model that recognizes that a radiative forcing at the surface must be compensated by atmospheric feedbacks governing the energy redistribution at the surface, which is brought about by the concomitant changes to important aerodynamic and physiological attributes:

$$\Delta T_s = \frac{\lambda_0}{1+f}\mathrm{RF}_{\alpha_s}^{\mathrm{SFC}} - \frac{\lambda_0}{(1+f)^2}R_N\Delta f \qquad (16)$$

where ΔT_s is the surface temperature change, $\mathrm{RF}_{\alpha_s}^{\mathrm{SFC}}$ is the radiative forcing at the surface due to changes in the surface albedo, λ_0 is the longwave radiation feedback ($1/(4\varepsilon_s\sigma T_s^3)$; with units °C(W m^{-2})$^{-1}$), and f is an energy 'redistribution efficiency' parameter that is largely determined by the intrinsic aerodynamic and physiological attributes of the vegetation:

$$f = \frac{\rho C_p}{4r_a\sigma T_s^3}\left(1+\frac{L(E+T)}{H}\right) \qquad (17)$$

where r_a is the bulk aerodynamic resistance [Eqn (8)], ρ is air density (kg m^{-3}), and C_p is the thermal inertia of air (J m^{-3} °C^{-1}). The surface temperature response following the external (albedo change) radiative forcing depends on the internal energy redistribution through convection and evapotranspiration, which in turn depends on the structural and physiological properties of the vegetation and on ambient environmental conditions (i.e., air temperature, humidity, and wind speed). These nonradiative factors are largely responsible for Δf and can be equally important in determining the overall local ΔT_s connected to FCC/FMC. In general, a higher value of f corresponds to a larger role played by the nonradiative feedback mechanisms [far right-hand term, Eqn (16)] and a lower local climate sensitivity to external ($\Delta\alpha_s$) radiative forcings. The nonradiative term in Eqn (16) (far right-hand term) can be expanded further for assessing the relative contribution of Bowen ratio and aerodynamic roughness changes [see (Lee *et al.*, 2011) for details].

Local air temperature change

Recall that radiative energy exposed to vegetation is transferred to the atmosphere by convection and evaporation of water (latent heat transfer), with consequent impacts on the surface radiative temperature, T_s. These energy transfers take place through a boundary layer with properties dependent on the viscosity of air and the transport of momentum from moving air to the vegetation surface (Monteith & Unsworth, 2008). As such, the amount of warming in the air (T_a) depends on the extent of turbulent mixing in the atmosphere, which is described by the depth of the atmospheric boundary layer (Oke, 2002). Due to their larger aerodynamic roughness properties, forests are more efficient at dissipating sensible heat away from the surface and into the boundary layer relative to open areas with shorter vegetation, particularly during the daytime (Hoffmann & Jackson, 2000; Lee *et al.*, 2011; Rotenberg & Yakir, 2011; Zhang *et al.*, 2014). At nighttime, however, some have argued that higher roughness properties can also serve to bring more heat from the nocturnal boundary layer down toward the surface layer relative to open areas (Lee *et al.*, 2011; Zhang *et al.*, 2014). As such, forests in many extra-tropical regions serve to warm local air temperatures over the diel (24 h) cycle [see, for example, Fig. 2 in Lee *et al.* (2011) and Fig. 4 in Zhang *et al.* (2014)]. Thus, due to atmospheric turbulence enhanced by vegetation, changes in the skin temperature of the surface (ΔT_s) may not always provide the best indication of the actual air temperature change, ΔT_a, following FCC/FMC.

Climate regulation index

West *et al.* (2011) developed 'climate regulation indices' (CRIs) that combined two dominant process influencing regional variations in climate: (i) the biogeophysical regulation of heat and moisture fluxes from local land surface processes and (ii) the advection (transport) of heat and moisture from large-scale atmospheric circulation. With the CRIs, the local surface energy and moisture balance impacts of LCC/FCC are scaled relative to the influence of advection, thus providing an indication of the importance of the vegetated land surface to local climate: as advection increases, the relevance of biophysical mechanisms (T_a in °C and moisture in mm) decreases.

The CRIs are presented in the form of high-resolution global maps. However, they were developed using the theoretical potential vegetation cover for each grid cell compared to bare ground/no vegetation cover are were not intended for use in routine climate impact assessments of FCC/FMC; thus, efforts would be required to

make them (or similar map-based metrics) more amenable to forest management contexts.

Climate regulation value

Anderson-Teixeira *et al.* (2012) quantified both biogeochemical and biogeophysical ecosystem climate services of 18 ecoregions across the Americas and combined them into a single indicator referred to as the 'climate regulation value' (CRV) that indexes the relative importance of biogeophysical to biogeochemical ecophysiological processes on land. CRV is essentially the time-integrated net change in global LW GHG forcing at TOA less the local surface energy balance change ($RF_{GHG} - \Delta R_N + \Delta L(E + T)$; in Watts per global m^2) relative to a pulse emission of CO_2 occurring in the year of LULCC.

The metric essentially combines the local direct biogeophysical climate effect (normalized to the area of the earth) with the global biogeochemical effect normalized to CO_2 as the common currency (to obtain units in 'CO_2-eq.'). 'Climate effect' here is simply the energy gained or removed from climate system at multiple levels of the atmosphere (surface and TOA). The metric does not account for the change in the surface (ΔT_s) or near-surface air temperatures (ΔT_a) which are of greater relevance to humans and to the functioning of local ecosystems (Pielke *et al.*, 2002; Betts, 2007). With the CRV metric, local nonradiative (i.e., from ΔH) and global radiative (i.e., from CO_2 RF) effects are summed, making meaningful interpretation difficult. Like the CRIs derived by West *et al.* (2011), the CRV of Anderson-Teixeira *et al.* (2012) was not intended as a metric for use in routine climate impact assessments of FCC/FMC.

Metric relationships

Figure 3 illustrates the principal direct biogeophysical forcing mechanisms at play following a vegetation perturbation on land and their associated climate metrics. $\Delta\alpha_s$ can be causally and linearly linked to $RF^{SFC}_{\Delta\alpha_s}$, $RF^{TOA}_{\Delta\alpha_s}$, $\Delta T_{a,\mathrm{global}}$, and any C-normalized metric through C eq.s (such as GWP or EESF/CDE). These metrics can be converted from each other, although the conversion factors and/or procedures differ from one analyst to another. Differences stem from the particular radiative transfer code used to convert $\Delta\alpha_s$to $RF^{TOA}_{\Delta\alpha_s}$ and in the climate sensitivity term (λ) required to convert from $RF^{TOA}_{\Delta\alpha_s}$ to $\Delta T_{\Delta\alpha_s}$ (shown as '$\Delta T_{a,\mathrm{global}}$' in Fig. 3).

While the $\Delta\alpha_s$metrics shown in Fig. 3 can be derived and converted from one to another with ease, local impacts such asΔT_a and ΔT_s cannot. This is owed to the nonlinear role of heat dissipation by surface roughness and evapotranspiration. Although ΔH and $\Delta L(E + T)$ are intimately linked to ΔT_s (Eqns (16) and (17)), ΔT_a is also affected by turbulent mixing and the dynamics of the atmospheric boundary layer (Oke, 2002; Baldocchi & Ma, 2013) and has no direct relationship with ΔT_s. Table 4 outlines the pros and cons of the metrics reviewed in this section.

Case studies

Environmental vs. biological controls

The role and importance of the local environmental controls (e.g., global radiation, precipitation, wind) may be just as important to quantify as the intrinsic biological properties of the vegetation itself (e.g., stomatal conductance, LAI, vegetation height), particularly when

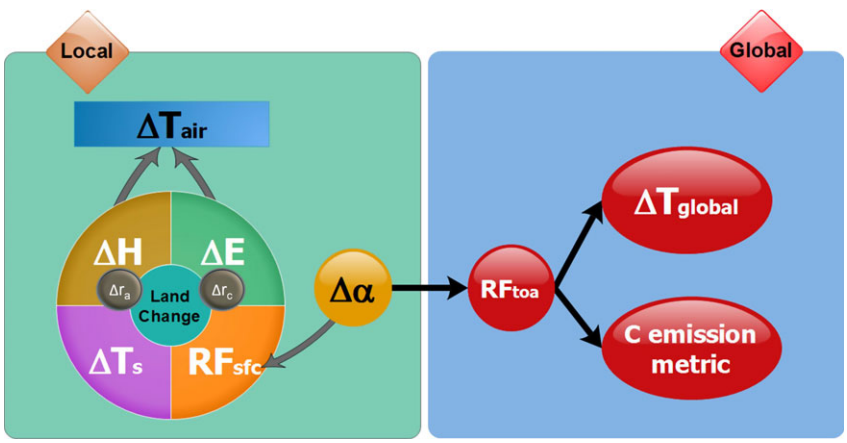

Fig. 3 Conceptual illustration of the relationships between the direct biogeophysical climate forcing mechanisms and corresponding metrics. 'E' = $L(E + T)$.

Table 4 Qualitative comparison of biogeophysical climate metrics for FCC/FMC

	Metric description	Unit	Pros	Cons
ΔR_N	Change in net radiation at the surface	Wm^{-2}	Relatively straightforward to compute	Does not convey information about the sign or magnitude of the temperature response
$-\frac{\lambda_0}{(1+f)^2} R_N \Delta f$	Local nonradiative forcing	°C	Informs of relative importance of r_a and $L(E + T)$ to $\Delta\alpha_s$	f is difficult to compute
$\frac{\lambda_0}{1+f} \mathrm{RF}^{\mathrm{SFC}}_{\alpha_s}$	Local radiative forcing at surface level	°C	Informs of relative importance of $\Delta\alpha_s$ to r_a and $L(E + T)$	f is difficult to compute
ΔT_s	Local surface temperature change	°C	A direct measure of the biogeophysical feedbacks on local climate; can be measured remotely	Not always in agreement with the local air temperature change (ΔT_a)
ΔT_a	Local near-surface air temperature change	°C	A more relevant measure of the climate feedbacks of FCC/FMC on local climate	Difficult to measure and quantify – requires additional modeling and/or assumptions
$\mathrm{RF}^{\mathrm{TOA}}_{\Delta\alpha_s}$	TOA radiative forcing from surface albedo changes	Wm^{-2}	Straightforward to compute; provides a basis for comparison with other climate forcing agents	Challenging to interpret by itself
$\Delta T_{\Delta\alpha_s}$	Global mean air temperature change from surface albedo changes	°C	More meaningful than $\mathrm{RF}^{\mathrm{TOA}}_{\Delta\alpha_s}$ in terms of policy relevancy	Cannot measure or quantify empirically; requires a model-derived climate sensitivity term (i.e., $\lambda_{\Delta\alpha_s}$; λ_{LCC})
$\mathrm{GWP}_{\Delta\alpha_s}$	Global warming potential from surface albedo changes	Kg-CO_2-eq. m^{-2}	Metric and units are familiar and can be easily integrated into existing accounting frameworks	Integrated measure that is context-specific; ignores local climate effect of $\Delta\alpha_s$
EESF/CDE	Emissions equivalent of shortwave forcing/carbon drawdown equivalent	T C-eq. ha^{-2}	Units are familiar and can be easily integrated into existing accounting frameworks	Does not include temporal dynamics of CO_2 and albedo; Ignores local climate effect of $\Delta\alpha_s$
CRV	Climate regulation value	Kg-CO_2-eq. m^{-2}	Showcases the relative importance of biogeophysical to biogeochemical climate regulation mechanisms of forested ecosystems	Combination of local surface and global TOA energy balance effects poses interpretation challenges
CRI	Climate regulation indices	mm-H_2O or °C	Indicates the contribution of local biogeophysical effects relative to atmospheric circulation	Difficult to quantify – requires knowledge of horizontal heat and moisture transport (advection)

management projects within or across regions having steep climate gradients are being compared. For any two forests having similar structural and physiological properties (i.e., LAI, h_c, g_s, *and* z_r), $\Delta\alpha_s$ will mostly be driven by differences in air temperature and precipitation as they affect snow cover and α_{sn} (when Δf_g and $\Delta\alpha_{g0}$ are assumed negligible), by differences in $R^{\downarrow}_{\mathrm{SW}}$ due to differences in latitude and atmospheric conditions (i.e., cloud cover, aerosol optical depth), and by differences in $\frac{H}{L(E+T)}$ (Bowen ratio) due to differences in humidity, precipitation, and wind speed. Understanding the role of environmental controls is relevant for the implementation of regionally optimized climate motivated forest management strategies and policies. Peng *et al.* (2014) showed that the benefits of afforestation in China (in terms of local ΔT_s relative to grassland or cropland) are likely to be enhanced in wetter regions ($P > 1200$ mm yr^{-1}) due to higher $L(E + T)$ and can even be counterproductive in dryer regions. For instance, the annual mean ΔT_s between plantation forests and open lands was found to be ~ −2 °C for regions experiencing $P > 1600$ mm $year^{-1}$ while ~ +2.5 °C for

regions experiencing P = 400–600 mm year^{-1} (Peng *et al.*, 2014).

Another example is in Norway, where coastal regions in the west are being considered for coniferous afforestation projects. The climate of the region is characterized as having much higher P and relatively milder annual mean air temperatures relative to the more traditional forestry regions in the east ($P \geq 3000$ vs. 500–1000 mm yr^{-1} and T = 6.3 C vs. 2.7 C, respectively) (Norwegian Meteorological Institute, 2013). Differences in these environmental controls result in a lower mean annual α_s and higher $L(E + T)$ in western Norway relative to forests of similar structure (basal area, LAI, dominant species) located in the cooler and dryer eastern regions. In terms of the biogeophysical feedbacks on local climate, afforestation projects in the western regions would warm T_s and cool T_a relative to similar afforestation projects in eastern regions of Norway, as illustrated in Table 5.

The importance of biological controls – or vegetation structure and physiology – become apparent when one compares sites sharing identical environmental controls (Table 5). The lower α_s of the coniferous relative to deciduous sites in both site-pair regions is attributed to a higher LAI during fall–spring months (Juang *et al.*, 2007; Bright *et al.*, 2014). In the SE USA during 2005, the lower α_s translated to higher radiation loads (R_N) and higher H fluxes, resulting in mean annual air and surface temperatures that were higher at the coniferous site relative to the deciduous site, despite having higher $L(E + T)$ (lower Bowen ratio) (Juang *et al.*, 2007). As for the Norwegian site comparison, despite having larger R_N loads at the coniferous site due in large part to its lower α_s, ΔT_s was much less pronounced between the two sites owed to the coniferous stand's larger surface roughness.

Forest management examples: temporary vs. permanent effects

Several of the metrics previously introduced are applied here to evaluate the climate change impacts of two realistic boreal forest management scenarios: (i) a clear-cut harvest and (ii) a species change. The first example is meant to illustrate the effects of rotation forestry in which the biogeophysical impacts are temporary, whereas the second example is meant to illustrate the more permanent nature of impacts resulting from – say – a strategy to

Table 5 Site pair comparison highlighting the role of environmental and biological controls on annual mean air and surface temperatures. Flux data for the USA are for 2005 and are adapted from Katul & Oren (2011a,b), and data from 2004 to 2009 for 'eastern Norway' (61.2 N, 12.4 E) are adapted from Bright *et al.* (2014). $L(E + T)$, α_s, and T_s for 'western Norway' (59.4 N, 6.1 E) are means over the same time period acquired from MODIS retrievals (ORNL DAAC, 2014). Radiation budget variables for 'western Norway' ($R^{\downarrow}_{SW}$; $R^{\downarrow}_{LW}$) are from NASA (2014)

Δ Definition	$\Delta\alpha_s$	$\Delta R^{\downarrow}_{SW}$[Wm^{-2}]	ΔR_N[Wm^{-2}]	$\Delta\frac{H}{L(E+T)}$, (Bowen Ratio)	ΔT_s[°C], Local	ΔT_a[°C], Local
Environmental control example						
Evergreen needleaf, western Norway – evergreen needleleaf, eastern Norway	−0.02 (= 0.10–0.12)	2 (= 113–111)	4 (= 50–46)	−0.8 (= 0.4–1.2)	1.4	−1.4† [H = 14 – H = 24]
Biological control examples						
Evergreen needleleaf, southeast USA – broadleaf deciduous, southeast USA	−0.04 (= 0.12–0.16)	0 (= 194–194)	12 (= 108–96)	−0.1 (= 0.39–0.44)	0.4*	0.3† [H = 30 – H = 28]
Evergreen needleleaf, eastern Norway – broadleaf deciduous, eastern Norway	−0.09 (= 0.12–0.21)	0 (=111–111)	7 (=46–39)	0.5 (= 1.2–0.8)	0.12	0.4† [H = 24 – H = 21]

*Calculated with $R^{\uparrow}_{LW}$ and an emissivity of 0.95.
†Calculated with a 12-h heating cycle and boundary layer mixing height of 250 m (West *et al.*, 2011).

suppress fire risk through a change in tree species (i.e., the replacement of coniferous forest with deciduous forest).

In the clear-cut example, the interannual time evolution of the monthly mean albedo changes following the harvest of a 100-year. spruce (*Picea abies*) and a 50-year birch (*Betula spp.*) stand is estimated with the empirical models of Bright *et al.* (2013), presented as the upper subpanels of Fig. 4.

The change in albedo, and thus the local instantaneous RF at the surface ($RF^{SFC}_{\Delta\alpha_s}$, blue curves, bottom panels, Fig. 4), is strongest immediately following the harvest disturbance, weakening rapidly over time as the canopy of the subsequent generation develops and starts to mask the snow-covered ground during months with snow cover. The time lag in the response by global mean temperature to the global $RF^{TOA}_{\Delta\alpha_s}$ is visible in Fig. 4; differences in magnitude of the temperature response are a product of the climate model and scenario in which the climate sensitivity parameter is derived. Differences in the global mean temperature response to RFs from L/FCC and $\Delta\alpha_{s,snow}$ reflect the differences in spatial heterogeneity between the two RFs as well as highlight the relevance and role of the nonradiative mechanisms in dampening the response to $RF^{SFC}_{\Delta\alpha_s}$ following LCC (or FCC).

As for $GWP_{\Delta\alpha_s}$ – an accumulated measure – the impact decreases with increasing TH due to the temporary nature (short lifetime) of $RF^{TOA}_{\Delta\alpha_s}$ relative to $RF^{TOA}_{CO_2}$ (Fig. 4, bottom, red). Following a clear-cut disturbance, EESF/CDE values are −23 and −11 t C-eq. ha^{-2} for the spruce and birch cases, respectively. To put this into perspective, typical aboveground C stocks in regional spruce and birch forests are around 30–40 t C ha^{-2} and 10–20 t C ha^{-2}, respectively. However, GWP values for spruce and birch when TH = 100 are 10 and 18% of the EESF/CDE values, respectively, illustrating the importance of understanding key calculation methods and

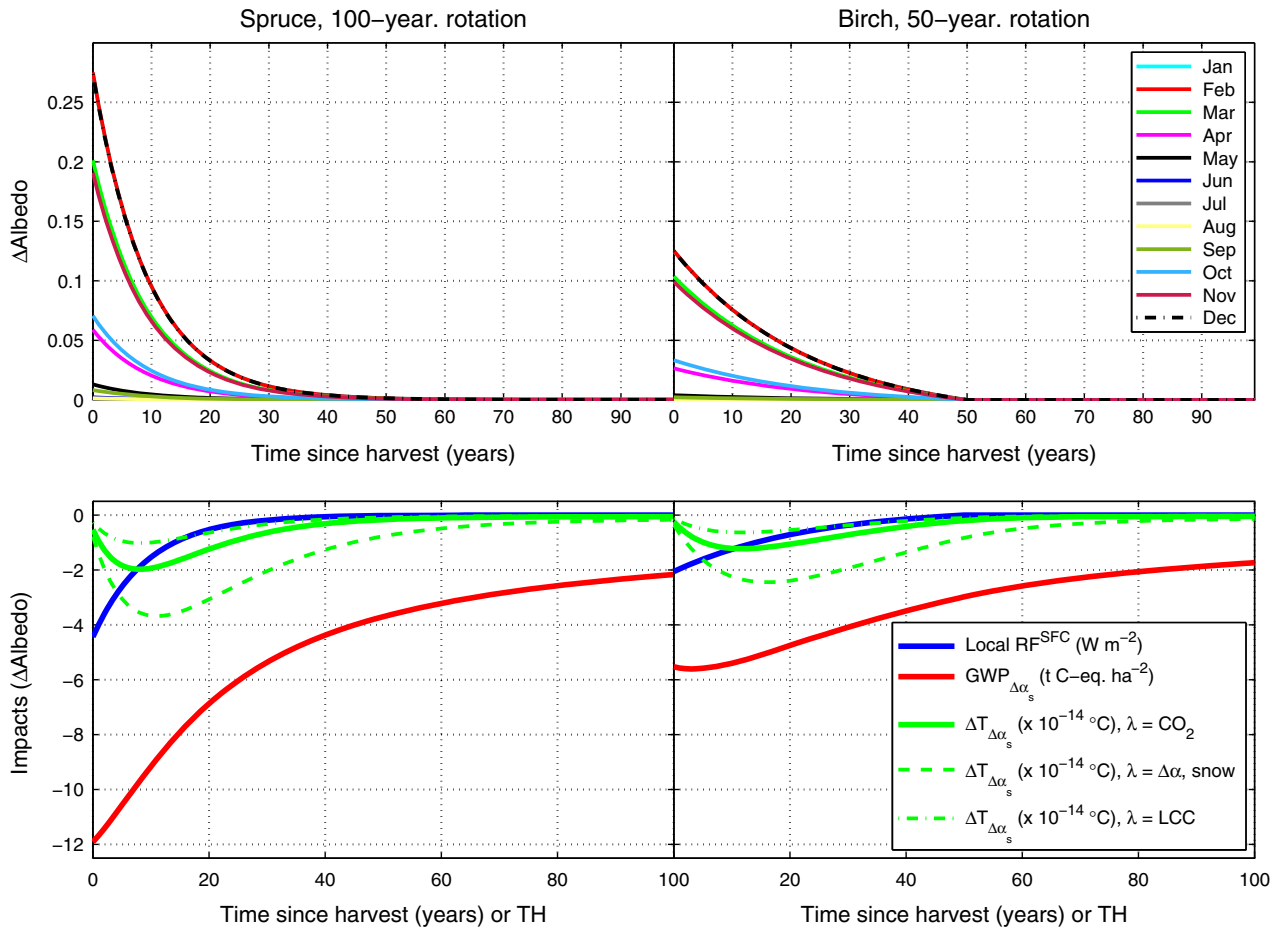

Fig. 4 (Upper panels) ΔAlbedo following a clear-cut harvest of typical spruce and birch stands in eastern Norway; (Lower panels) The associated climate impact as quantified with different metric alternatives. Three global mean temperature responses are presented: one using the equilibrium climate sensitivity (λ) for 2 × CO_2 (Boucher & Reddy, 2008), a second for a 5% decrease in land snow albedo (Bellouin & Boucher, 2010), and a third for global historical LCC (Davin *et al.*, 2007).

assumptions behind albedo metrics expressed in units of C (or CO_2) equivalents, particularly if they are ever to be integrated in greenhouse accounting frameworks. For instance, the accumulated RF of 23 t C-eq. ha^{-2} (the value of the EESF/CDE for the spruce case) when modeled as an actual CO_2 emission pulse (after converting to CO_2) is an order of magnitude larger than the accumulated $RF^{TOA}_{\Delta\alpha_s}$ after 100 years (TH = 100; −7.7 e-13 vs. −7.7e-14 W yr m^{-2}, respectively).

As for the second example in which a harvested spruce stand is regenerated with birch and left untouched for 100 years, the higher albedo of birch relative to spruce in all months results in positive monthly albedo changes ($\Delta\alpha_s$, Fig. 5 left) and negative annual mean $RF^{SFC}_{\Delta\alpha_s}$ (Fig. 5 middle) that persists over the entire analytical period. The local surface temperature response from the change in albedo (Fig. 5, middle, dashed cyan) is offset by a slight warming from the change in nonradiative mechanisms (Fig. 5, middle, dashed red) although the albedo contribution largely dictates the net ΔT_s response (Fig. 5, middle, magenta). The nonradiative warming contribution is dominated by the lower surface roughness (z_0) and higher aerodynamic resistance (r_a) of birch, which more than offsets the nonradiative cooling from its lower Bowen ratio (higher $L(E + T)$).

As for the global impact of the albedo change (Fig. 5, right panel), the permanent nature of the instantaneous $RF^{TOA}_{\Delta\alpha_s}$ results in a permanent $\Delta T_{\Delta\alpha_s}$ whose magnitude again depends on the chosen climate sensitivity. Unlike the temporary case, $GWP_{\Delta\alpha_s}$ values here increase in magnitude with increasing metric TH. Other management actions leading to permanent changes in surface biogeophysical properties such as the afforestation of croplands or grasslands, for example, would also result in a permanent $\Delta T_{\Delta\alpha_s}$ and large $GWP_{\Delta\alpha_s}$ values that increase in magnitude with increasing TH.

Locally, the permanent biogeophysical impact from spruce afforestation can be gauged if one compares the biogeophysical attributes of a clear-cut site to the mature spruce site, shown in Table 6.

Although the clear-cut site is not directly comparable to the type of lands typically considered in afforestation projects (i.e., croplands and pastures), it does provide a

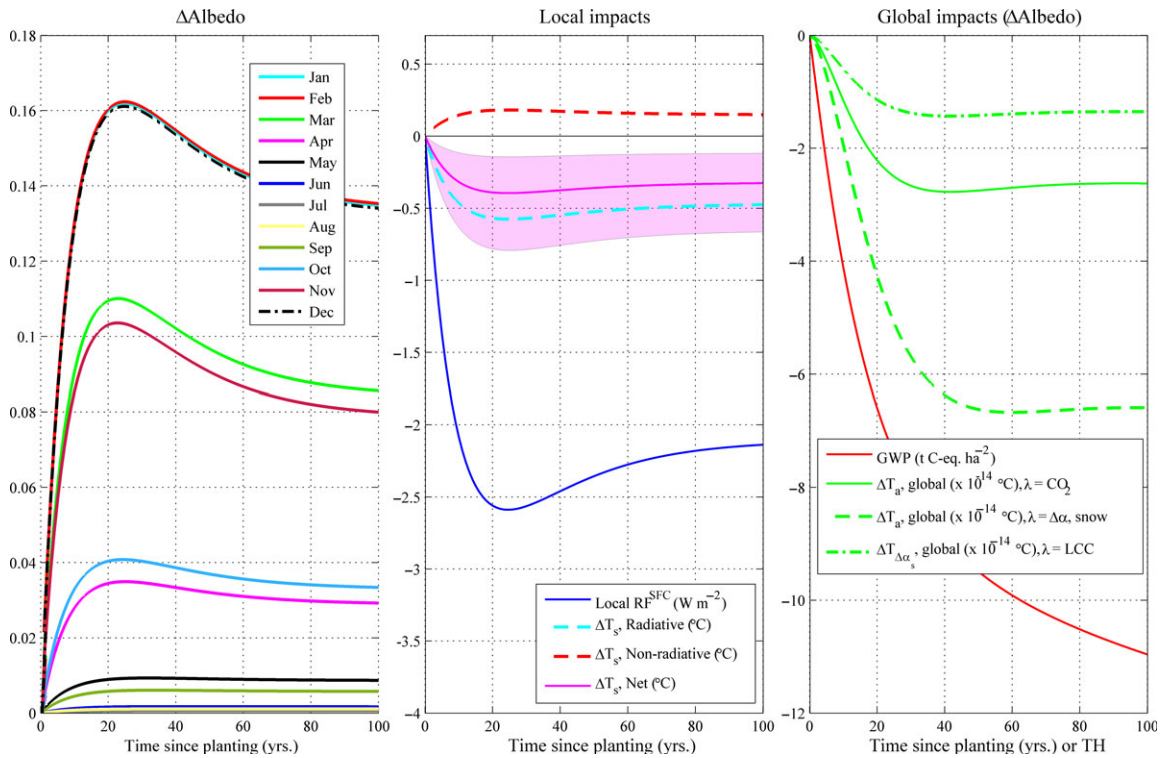

Fig. 5 Direct biogeophysical impacts of a change in tree species in boreal Norway. (Left) Changes in the monthly mean albedo when replacing spruce with birch over 100 years; (Middle) Local surface shortwave forcing ($RF^{SFC}_{\Delta\alpha_s}$) and the local surface temperature response (ΔT_s; magenta curve) decomposed into radiative (dashed cyan) and nonradiative components (dashed red curve). ΔT_s (t) is approximated with Eqn (16) based on the information presented in Table 6 and the ratio of annual mean radiative to nonradiative forcings. December and April net ΔT_s make up the upper and lower ranges of the annual mean net ΔT_s, respectively; (Right) Global impacts from the albedo changes.

Table 6 2004–2007 mean surface energy balance indicators of a boreal forest site cluster in eastern Norway (Bright *et al.*, 2014). The 3-year mean ΔT_s between the three sites is estimated with Eqn (16) and a 3-year annual mean for $R_{SW}^{\downarrow}$ and λ_0 of 109 Wm^{-2} and 0.23 K $(Wm^{-2})^{-1}$, respectively

	α_s	$\Delta\frac{H}{L(E+T)}$	$R_N[Wm^{-2}]$	$H[Wm^{-2}]$	$L(E+T)[Wm^{-2}]$	f	z_0[m]	$r_a[sm^{-2}]$
Birch	0.21	0.9	43	20	22	5.0	1.4	68
Spruce	0.11	1.1	46	24	21	5.5	2.1	56
Clear-cut	0.26	1.2	41	20	17	3.8	0.7	80
	$\frac{\lambda_0}{1+f}RF_{\alpha_s}^{SFC}$ (°C, Radiative)		$-\frac{\lambda_0}{(1+f)^2}R_N\Delta f$ (°C, Nonradiative)		ΔT_s, Net (°C)			
Open to Spruce	0.61		−0.42		0.19			
Spruce to Birch	−0.42		0.11		−0.31			

sense of the evergreen forest's role in regulating local climate. As seen in Table 6, the lower albedo dominates the net ΔT_s despite the nonradiative cooling from evapotranspiration and aerodynamic roughness. Even though afforestation results in an increase in the latent heat flux $L(E + T)$, the sensible heat flux H is also increased. We can approximate an annual mean ΔT_a of 0.56 °C from the 4 Wm^{-2} increase in H by assuming a boundary layer mixing height of 250 m and a 12-h heating cycle representative of the global annual mean (West *et al.*, 2011).

Research needs and future directions

Climate sensitivity and RF efficacy

In recent years, radiative forcing contributions from $\Delta\alpha_s$ have been increasingly included in climate impact assessment studies. Yet the extent to which a $RF_{\Delta\alpha_s}^{TOA}$ from local $\Delta\alpha_s$ affects the global mean surface temperature is complicated, particularly when compared to the global forcing from well-mixed CO_2. The climate sensitivity λ depends on the spatial distribution of the RF (Joshi *et al.*, 2003; Hansen & Nazarenko, 2004; Hansen *et al.*, 2005). Temperature responses to RFs at high latitudes can be over four times greater in magnitude than those at low latitudes owed to the stimulation of positive snow/ice albedo feedbacks and to the relative stability of the atmospheric temperature profile at high latitudes (Hansen *et al.*, 1997, 2005; Forster *et al.*, 2000; Joshi *et al.*, 2003; Hansen & Nazarenko, 2004). This has given rise to RF adjustments with a factor sometimes referred to as climate 'efficacy' (Hansen *et al.*, 2005), which is defined as the ratio of λ for some forcing agent relative to that for CO_2.

Estimates of climate sensitivity and radiative forcing efficacy from FCC/FMC vary widely in the literature (Table 7). Recall from Eq. (16) and Fig. 5 that the nonradiative internal feedbacks from FCC/FMC can dampen the externally driven radiative temperature changes (Davin & De Noblet-Ducoudré, 2010; Lee *et al.*, 2011). For these reasons, Davin *et al.* (2007) report a λ connected to historical global land-use changes (LCC) of 0.52 °C$(Wm^{-2})^{-1}$ yielding an efficacy of 0.5. Hansen *et al.* (2005), however, report an efficacy of 1.02 for their global historical LCC simulations using the same vegetation maps [i.e., (Ramankutty & Foley, 1999)], which demonstrates the dependency of λ (and efficacies) on the particular climate model from which they are derived.

Table 7 Reported global climate sensitivities (λ_{α_s}; °C $(Wm^{-2})^{-1}$) and efficacies ($\lambda_{\alpha_s}/\lambda_{CO_2}$; Unitless) for $RF_{\Delta\alpha_s}^{TOA}$ (Wm^{-2})

Model	λ, $RF_{\Delta\alpha_s}^{TOA}$ (LCC)	Efficacy	Reference
IPSL-CM4	0.52	0.5	(Davin *et al.*, 2007)
IPSL	0.93*	0.78	(Davin & De Noblet-Ducoudré, 2010)
GISS E vIII	0.45	1.02	(Hansen *et al.*, 2005)
IAP RAS CM	0.49	N/A	(Eliseev, 2011)
CCSM4 v8	0.62	0.79	(Jones *et al.*, 2013)
CCSM4 v4	0.36†	N/A	(Lawrence *et al.*, 2012)

*FCC only; †$\Delta T_a/RF_{\Delta\alpha_s}^{SFC}$.

Davin & De Noblet-Ducoudré (2010) report a λ of 0.93 °C$(Wm^{-2})^{-1}$ in a more recent modeling study limited to global-scale deforestation (FCC) illustrating that – to some extent – the spread in λ (and efficacy) seen in the literature can also stem from the type of vegetation changes that are modeled.

Jones *et al.* (2013) showed that RFs from well-mixed GHGs like CO_2 and those from LCC ($\Delta\alpha_s$) – even if adjusted with efficacies – do not produce the same global temperature response when added together, in part because of spatial heterogeneity, nonradiative effects, and other factors. They argue instead that it is the indi-

vidual climate responses that should be added directly. This argument should not detract from efforts to move down the cause–effect chain from $\Delta\alpha_s$to $RF^{TOA}_{\Delta\alpha_s}$. The metric $RF^{TOA}_{\Delta\alpha_s}$ provides information about the net energy gained or lost from the climate system and can be quantified for stand-level perturbations, whereas a global temperature response cannot. Sustained efforts by the climate modeling community to quantify and build consensus on regional responses to $RF^{TOA}_{\Delta\alpha_s}$ from different kinds of FCC/FMC would allow nonclimate modelers the opportunity characterize temperature impacts with a higher degree of certainty.

Summary and recommendations

Biogeophysical factors associated with forestry activities – including albedo and turbulent heat exchange – are rarely considered by policymakers, despite the fact that such factors can affect local climate in ways counter to carbon sequestration. Researchers need to assist policymakers if they are to move beyond a strictly carbon-centric accounting framework for forest mitigation activities. Inclusion of global mean impacts from albedo change RFs are an improvement but fall short of a full biophysical accounting. Forestry impacts on local T_a are often more important than effects on the mean global T_a, despite the challenges associated with quantifying them or inferring them from paired site cluster measurements as air, as a fluid, is highly dynamic and unpredictable. For analyses at the site level, it is often easier to justify taking the difference between surface biophysical variables as they impact vertical heat exchanges (i.e., $L(E + T)$, H) and T_s because they are directly determined by the canopy–ground composites (i.e., the structural, physiological, and environmental controls).

Metrics based on RF will have greater policy relevance if appropriate adjustments are made to account for differences in the local/regional response by temperature from differences in the nonradiative mechanisms responsible for the internal feedbacks. This approach requires sustained efforts by coupled climate modelers to quantify regional climate sensitivities and by micrometeorologists to quantify the energy redistribution efficiency parameter f (see Eqn 13) for a variety of forest types and other terrestrial ecosystems. Gridded maps of f for major forest biomes would facilitate identification of regions in which the nonradiative mechanisms warrant explicit consideration in climate impact assessment studies or policies. Albedo radiative forcings dominate climate feedbacks when values of f are low, for example.

The differences between local and global effects are relevant for mitigation activities involving forestry. The net radiative forcing to date from CO_2 emissions accompanying global deforestation is ~ 0.4 W m^{-2}; the accompanying global effect of increased surface albedo is about −0.2 W m^{-2}, but the local albedo effect can be two orders or magnitude greater – as much as ~ 20 W m^{-2} in boreal and arid temperate forests, for instance (Betts *et al.*, 2007b; Rotenberg & Yakir, 2010, 2011; Houspanossian *et al.*, 2013). Thus, some forestry activities will cool globally while warming the land surface locally. Similarly, the increased evapotranspiration of forests compared to grasslands or croplands often cools the land surface locally. Globally, the direct effect of increased $L(E + T)$ is less clear as the net global energy balance will effectively be zero when the water condenses elsewhere. However, if the extra water vapor increases cloud cover, then a cooling factor may be introduced indirectly due to enhancements in atmospheric albedo (Ban-Weiss *et al.*, 2011). A small warming factor is also introduced because water is a potent greenhouse gas. Determining the net effect of these interactions remains difficult and requires both meso- and global-scale models. Quantifying and attributing indirect impact mechanisms to specific forestry and other land-use activities should be a future research priority.

As for the direct biogeophysical climate forcings connected to land use and land management, we have reviewed and identified different approaches and metrics to quantify them. We have also recommended research priorities to help overcome some of the challenges associated with measuring radiative and nonradiative forcings. Such knowledge should help build bridges among the climate modeling, forest ecology, and resource management communities and, ultimately, allow us to include all direct biogeophysical forcings in our estimates of the climate benefits of different land-use activities.

Acknowledgements

This work was performed under the project 'Approaches for integrated assessment of forest ecosystem services under large scale bioenergy utilization' funded by the Norwegian Research Council (grant number: 233641/E50). Additional funding has been provided by USDA-AFRI (grant number: 2012-00857).

References

Abiodun BJ, Pal JS, Afiesimama EA, Gutowski WJ, Adedoyin A (2008) Simulation of West African monsoon using RegCM3 Part II: impacts of deforestation and desertification. *Theoretical and Applied Climatology*, **93**, 245–261.

Allen RG, Jensen ME, Wright JL, Burman RD (1989) Operational estimates of reference evapotranspiration. *Agronomy Journal*, **81**, 650–662.

Allen RG, Pereira LS, Raes D, Smith M (1998) Crop evapotranspiration - Guidelines for computing crop water requirements - FAO irrigation and drainage paper 56. Rome, Italy, UN. FAO.

Anderson-Teixeira K, Snyder P, Twine T, Cuadra S, Costa M, Delucia E (2012) Climate-regulation services of natural and agricultural ecoregions of the Americas. *Nature Climate Change*, **2**, 177–181.

Anderson RG, Canadell JG, Randerson JT *et al.* (2010) Biophysical considerations in forestry for climate protection. *Frontiers in Ecology & Environment*, **9**, 174–182.

Arneth A, Sitch S, Bondeau A *et al.* (2010) From biota to chemistry and climate: towards a comprehensive description of trace gas exchange between the biosphere and atmosphere. *Biogeosciences*, **7**, 121–149.

Arora VK, Montenegro A (2011) Small temperature benefits provided by realistic afforestation efforts. *Nature Geoscience*, **4**, 514–518.

Avissar R, Werth D (2005) Global hydroclimatological teleconnections resulting from tropical deforestation. *Journal of Hydrometeorology*, **6**, 134–145.

Bala G, Caldeira K, Wickett M, Phillips TJ, Lobell DB, Delire C, Mirin A (2007) Combined climate and carbon-cycle effects of large-scale deforestation. *PNAS*, **104**, 6550–6555.

Baldocchi D, Ma S (2013) How will land use affect air temperature in the surface boundary layer? Lessons learned from a comparative study on the energy balance of an oak savanna and annual grassland in California, USA. Tellus B; Vol 65 (2013).

Ban-Weiss GA, Bala G, Cao L, Pongratz J, Caldeira K (2011) Climate forcing and response to idealized changes in surface latent and sensible heat. *Environmental Research Letters*, **6**, 034032.

Bartlett PA, Mackay MD, Verseghy DL (2006) Modified snow algorithms in the Canadian land surface scheme: model runs and sensitivity analysis at three boreal forest stands. *Atmosphere-Ocean*, **44**, 207–222.

Bellouin N, Boucher O (2010) Climate response and efficacy of snow albedo forcings in the HadGEM2-AML climate model. Hadley Centre Technical Note, HCTN82. UK Met Office.

Betts AK, Ball JH (1997) Albedo over the boreal forest. *Journal of Geophysical Research*, **102**, 28901–28909.

Betts AK, Desjardins RL, Worth D (2007a) Impact of agriculture, forest and cloud feedback on the surface energy budget in BOREAS. *Agricultural and Forest Meteorology*, **142**, 156–169.

Betts R (2007) Implications of land ecosystem-atmosphere interactions for strategies for climate change adaptation and mitigation. *Tellus Series B*, **59**, 602–615.

Betts R, Falloon PD, Goldewijk KK, Ramankutty N (2007b) Biogeophysical effects of land use on climate: model simulations of radiative forcing and large-scale temperature change. *Agricultural and Forest Meteorology*, **142**, 216–233.

Betts RA (2000) Offset of the potential carbon sink from boreal forestation by decreases in surface albedo. *Nature*, **408**, 187–190.

Boisier JP, De Noblet-Ducoudré N, Pitman AJ *et al.* (2012) Attributing the impacts of land-cover changes in temperate regions on surface temperature and heat fluxes to specific causes: results from the first LUCID set of simulations. *Journal of Geophysical Research: Atmospheres*, **117**, D12116.

Bonan GB (2002) *Ecological Climatology: Concepts and Applications*. Cambridge University Press, Cambridge, UK.

Bonan GB (2008) Forests and climate change: forcings, feedbacks, and the climate benefits of forests. *Science*, **320**, 1444–1449.

Boucher O, Reddy MS (2008) Climate trade-off between black carbon and carbon dioxide emissions. *Energy Policy*, **36**, 193–200.

Bright RM, Kvalevåg MM (2013) Technical note: evaluating a simple parameterization of radiative shortwave forcing from surface albedo change. *Atmospheric Chemistry and Physics*, **13**, 11169–11174.

Bright RM, Astrup R, Strømman AH (2013) Empirical models of monthly and annual albedo in managed boreal forests of interior Norway. *Climatic Change*, **120**, 183–196.

Bright RM, Antón-Fernández C, Astrup R, Cherubini F, Kvalevåg MM, Strømman AH (2014) Climate change implications of shifting forest management strategy in a boreal forest ecosystem of Norway. *Global Change Biology*, **20**, 607–621.

Bright RM (2015a) Metrics for biogeophysical climate forcings from land use and land cover changes and their inclusion in life cycle assessment: a critical review. *Environmental Science & Technology*, **49**, 3291–3303.

Bright RM, Myhre G, Astrup R, Antón-Fernández C, Strømman AH (2015b) Radiative forcing bias of simulated surface albedo modifications linked to forest cover changes at northern latitudes. *Biogeosciences*, **12**, 2195–2205.

Caiazzo F, Malina R, Staples MD, Wolfe PJ, Yim SH, Barrett SR (2014) Quantifying the climate impacts of albedo changes due to biofuel production: a comparison with biogeochemical effects. *Environmental Research Letters*, **9**, 024015.

Cess RD (1978) Biosphere-albedo feedback and climate modeling. *Journal of the Atmospheric Sciences*, **35**, 1765–1768.

Chapin IiiFS, Matson PA, Vitousek P (2012) *Principles of Terrestrial Ecosystem Ecology*, 2nd Ed. Springer, New York, NY, USA.

Chen G-S, Notaro M, Liu Z, Liu Y (2012) Simulated local and remote biophysical effects of afforestation over the Southeast United States in boreal summer*. *Journal of Climate*, **25**, 4511–4522.

Cherubini F, Bright RM, Strømman AH (2012) Site-specific global warming potentials of biogenic CO2 for bioenergy: contributions from carbon fluxes and albedo dynamics. *Environmental Research Letters*, **7**, 045902.

Colaizzi PD, Evett SR, Howell TA, Tolk JA (2004) Comparison of aerodynamic and radiometric surface temperature using precision weighing lysimeters.

Cotton WR, Pielke RA (1995) *Human Impacts on Weather and Climate*. Cambridge University Press, Cambridge, UK; New York, NY, USA; Melbourne, Australia.

Davin EL, De Noblet-Ducoudré N (2010) Climatic impact of global-scale deforestation: radiative versus nonradiative processes. *Journal of Climate*, **23**, 97–112.

Davin EL, De Noblet-Ducoudré N, Friedlingstein P (2007) Impact of land cover change on surface climate: relevance of the radiative forcing concept. *Geophysical Research Letters*, **34**, L13702.

Deardorff JW (1978) Efficient prediction of ground surface temperature and moisture, with inclusion of a layer of vegetation. *Journal of Geophysical Research*, **83**, 1889–1903.

De Noblet-Ducoudré N, Boisier J-P, Pitman A *et al.* (2012) Determining robust impacts of land-use-induced land cover changes on surface climate over North America and Eurasia: results from the first set of LUCID experiments. *Journal of Climate*, **25**, 3261–3281.

Devaraju N, Bala G, Nemani R (2015) Modelling the influence of land-use changes on biophysical and biochemical interactions at regional and global scales. *Plant, Cell & Environment*, DOI: 10.1111/pce.12488.

Dickinson RE (1983) Land surface processes and climate-surface albedos and energy balance. *Advances in Geophysics*, **25**, 305–353.

Ding R, Kang S, Du T, Hao X, Zhang Y (2014) Scaling up stomatal conductance from leaf to canopy using a dual-leaf model for estimating crop evapotranspiration. *PLoS One*, **9**, e95584.

Durieux L, Machado LAT, Laurent H (2003) The impact of deforestation on cloud cover over the Amazon arc of deforestation. *Remote Sensing of Environment*, **86**, 132–140.

Eliseev AV (2011) Comparison of climatic efficiency of the mechanisms of land-surface albedo changes caused by land use, Izvestiya. *Atmospheric and Oceanic Physics*, **47**, 290–300.

Essery R (2013) Large-scale simulations of snow albedo masking by forests. *Geophysical Research Letters*, **40**, 5521–5525.

Essery R, Rutter N, Pomeroy JW *et al.* (2009) SnowMIP2: an evaluation of forest snow process simulations. *Bulletin of the American Meteorological Society*, **August**, 1–16.

FAO, JRC (2012) Global forest land-use change 1990–2005. *FAO Forestry Paper N. 169, Food and Agriculture Organization of the United Nations and European Commission Joint Research Centre* (eds Lindquist EJ, D'annunzio R, Gerrand A, Macdicken K, Achard F, Beuchle R, Brink A, Eva HD, Mayaux P, San-Miguel-Ayanz J, Stibig H-J), pp. 45. FAO, Rome, Italy.

Feddema JJ, Oleson KW, Bonan GB, Mearns LO, Buja LE, Meehl GA, Washington WM (2005) The importance of land-cover change in simulating future climates. *Science*, **310**, 1674–1678.

Foley JA, Costa MH, Delire C, Ramankutty N, Snyder P (2003) Green surprise? How terrestrial ecosystems could affect earth's climate. *Frontiers in Ecology and the Environment*, **1**, 38–44.

Forster PM, Blackburn M, Glover R, Shine KP (2000) An examination of climate sensitivity for idealised climate change experiments in an intermediate general circulation model. *Climate Dynamics*, **16**, 833–849.

Goldewijk KK (2001) Estimating global land use change over the past 300 years: the HYDE Database. *Global Biogeochemical Cycles*, **15**, 417–433.

Hansen J, Nazarenko L (2004) Soot climate forcing via snow and ice albedos. *Proceedings of the National Academy of Sciences of the United States of America*, **101**, 423–428.

Hansen J, Sato M, Ruedy R (1997) Radiative forcing and climate response. *Journal of Geophysical Research: Atmospheres*, **102**, 6831–6864.

Hansen J, Sato M, Ruedy R *et al.* (2005) Efficacy of climate forcings. *Journal of Geophysical Research: Atmospheres*, **110**, D18104.

Hedstrom NR, Pomeroy JW (1998) Measurements and modelling of snow interception in the boreal forest. *Hydrological Processes*, **12**, 1611–1625.

Henderson-Sellers A, Wilson MF (1983) Albedo observations of the earth's surface for climate research. *Philosophical Transactions of the Royal Society of London. B*, **309**, 285–294.

Hoffmann WA, Jackson RB (2000) Vegetation-climate feedbacks in the conversion of tropical Savanna to grassland. *Journal of Climate*, **13**, 1593–1602.

Hollinger DY, Ollinger SV, Richardson AD *et al*. (2010) Albedo estimates for land surface models and support for a new paradigm based on foliage nitrogen concentration. *Global Change Biology*, **16**, 696–710.

Houspanossian J, Nosetto M, Jobbágy EG (2013) Radiation budget changes with dry forest clearing in temperate Argentina. *Global Change Biology*, **19**, 1211–1222.

Idso SB, Jackson RD, Reginato RJ, Kimball BA, Nakayama FS (1975) The dependence of bare soil albedo on soil water content. *Journal of Applied Meteorology*, **14**, 109–113.

Irmak S, Mutiibwa D, Irmak A, Arkebauer TJ, Weiss A, Martin DL, Eisenhauer DE (2008) On the scaling up leaf stomatal resistance to canopy resistance using photosynthetic photon flux density. *Agricultural and Forest Meteorology*, **148**, 1034–1044.

Jackson RB, Randerson JT, Canadell JG *et al*. (2008) Protecting climate with forests. *Environmental Research Letters*, **3**, 044006. (044005 pp).

Jones AD, Collins WD, Torn MS (2013) On the additivity of radiative forcing between land use change and greenhouse gases. *Geophysical Research Letters*, **40**, 4036–4041.

Joos F, Roth R, Fuglestvedt JS *et al*. (2013) Carbon dioxide and climate impulse response functions for the computation of greenhouse gas metrics: a multi-model analysis. *Atmospheric Chemistry and Physics*, **13**, 2793–2825.

Joshi M, Shine K, Ponater M, Stuber N, Sausen R, Li L (2003) A comparison of climate response to different radiative forcings in three general circulation models: towards an improved metric of climate change. *Climate Dynamics*, **20**, 843–854.

Juang J-Y, Katul G, Siqueira M, Stoy P, Novick K (2007) Separating the effects of albedo from eco-physiological changes on surface temperature along a successional chronosequence in the southeastern United States. *Geophysical Research Letters*, **34**, L21408.

Katul G, Oren R (2011a) Duke forest hardwoods flux data. AmeriFlux Site and Data Exploration System. Available at: http://ameriflux.ornl.gov/ (accessed 5 January 2015).

Katul G, Oren R (2011b) Duke forest loblolly pine ameri-flux data. AmeriFlux Site and Data Exploration System. Available at: http://ameriflux.ornl.gov/ (accessed 5 January 2015).

Kelliher FM, Leuning R, Raupach MR, Schulze ED (1995) Maximum conductances for evaporation from global vegetation types. *Agricultural and Forest Meteorology*, **73**, 1–16.

Kirschbaum MUF, Whitehead D, Dean SM, Beets PN, Shepherd JD, Ausseil A-GE (2011) Implications of albedo changes following afforestation on the benefits of forests as carbon sinks. *Biogeosciences*, **8**, 3687–3696.

Klingaman NP, Butke J, Leathers DJ, Brinson KR, Nickl E (2008) Mesoscale simulations of the land surface effects of historical logging in a moist continental climate regime. *Journal of Applied Meteorology and Climatology*, **47**, 2166–2182.

Lawrence PJ, Feddema JJ, Bonan GB *et al*. (2012) Simulating the biogeochemical and biogeophysical impacts of transient land cover change and wood harvest in the community climate system model (CCSM4) from 1850 to 2100. *Journal of Climate*, **25**, 3071–3095.

Lee X, Goulden ML, Hollinger DY *et al*. (2011) Observed increase in local cooling effect of deforestation at higher latitudes. *Nature*, **479**, 384–387.

Lohila A, Minkkinen K, Laine J *et al*. (2010) Forestation of boreal peatlands: impacts of changing albedo and greenhouse gas fluxes on radiative forcing. *Journal of Geophysical Research: Biogeosciences*, **115**, 1–15.

Luyssaert S, Jammet M, Stoy P *et al*. (2014) Land management and land-cover change have impacts of similar magnitude on surface temperature. *Nature Climate Change*, **4**, 389–393.

Mahmood R, Pielke RA, Hubbard KG *et al*. (2013) Land cover changes and their biogeophysical effects on climate. *International Journal of Climatology*, **34**, 929–953.

Mahmood R, Quintanar AI, Conner G *et al*. (2010) Impacts of land use/land cover change on climate and future research priorities. *Bulletin of the American Meteorological Society*, **91**, 37–46.

Mcguire AD, Chapin FS, Walsh JE, Wirth C (2006) Integrated regional changes in arctic climate feedbacks: implications for the global climate system. *Annual Review of Environment and Resources*, **31**, 61–91.

Meyfroidt P, Rudel TK, Lambin EF (2010) Forest transitions, trade, and the global displacement of land use. *Proceedings of the National Academy of Sciences*, **107**, 20917–20922.

Mohr KI, David Baker R, Tao W-K, Famiglietti JS (2003) The sensitivity of West African convective line water budgets to land cover. *Journal of Hydrometeorology*, **4**, 62–76.

Monteith JL (1965) Evaporation and environment. *Symposia of the Society for Experimental Biology*, **19**, 205–224.

Monteith JL, Unsworth MH (eds.) (2008) *Principles of Environmental Physics*. Elsevier Academic Press, London.

Montenegro A, Eby M, Mu Q, Mulligan M, Weaver AJ, Wiebe EC, Zhao M (2009) The net carbon drawdown of small scale afforestation from satellite observations. *Global and Planetary Change*, **69**, 195–204.

Mu Q, Zhao M, Running SW (2011) Improvements to a MODIS global terrestrial evapotranspiration algorithm. *Remote Sensing of Environment*, **115**, 1781–1800.

Muñoz I, Campra P, Fernández-Alba AR (2010) Including CO2-emission equivalence of changes in land surface albedo in life cycle assessment. Methodology and case study on greenhouse agriculture. *International Journal of Life Cycle Assessment*, **15**, 672–681.

Murry FW (1967) On the computation of saturation vapor pressure. *Journal of Applied Meteorology*, **6**, 203–204.

Myhre G, Highwood EJ, Shine KP, Stordal F (1998) New estimtes of raditive forcing due to well mixed greenhouse gases. *Geophysical Research Letters*, **25**, 2715–2718.

Nakai T, Sumida A, Daikoku K *et al*. (2008) Parameterisation of aerodynamic roughness over boreal, cool- and warm-temperate forests. *Agricultural and Forest Meteorology*, **14**, 1916–1925.

NASA ASDC (2014) NASA/GEWEX Solar Radiation Budget (SRB) data, release v.3.0. Available at: https://eosweb.larc.nasa.gov/project/srb/srb_table (accessed 18 November 2014). NASA Atmospheric Science and Data Center.

Niu G-Y, Yang Z-L (2004) Effects of vegetation canopy processes on snow surface energy and mass balances. *Journal of Geophysical Research: Atmospheres*, **109**, D23111.

Norwegian Meteorological Institute (2013) eKlima - Monthly historical meteorology. Norwegian Meteorological Institute. Available at: http://sharki.oslo.dnmi.no/portal/page?_pageid=73,39035,73_39049&_dad=portal&_schema=PORTAL (accessed 31 January 2013).

Oke TR (2002) *Boundary Layer Climates*. Taylor & Francis e-Library, London, UK.

Ollinger SV, Richardson AD, Martin ME *et al*. (2008) Canopy nitrogen, carbon assimilation, and albedo in temperate and boreal forests: functional relations and potential climate feedbacks. *Proceedings of the National Academy of Sciences*, **105**, 19336–19341.

ORNL DAAC (2014) MODIS subsetted land products, collection 5. Available at [http://daac.ornl.gov/MODIS/modis.html] from ORNL DAAC, Oak Ridge, Tennessee, USA. (accessed 28 November 2014). Oak Ridge National Laboratory Distributed Active Archive Center (ORNL DAAC).

Otterman J (1977) Anthropogenic impact on the albedo of the earth. *Climatic Change*, **1**, 137–155.

Peng S-S, Piao S, Zeng Z *et al*. (2014) Afforestation in China cools local land surface temperature. *Proceedings of the National Academy of Sciences*, **111**, 2915–2919.

Pereira LS, Perrier A, Allen RG, Alves I (1999) Evapotranspiration: concepts and future trends. *Journal of Irrigation and Drainage Engineering*, **125**, 45–51.

Perrier A (1982) Land surface processes: vegetation. In: *Land Surface Processes in Atmospheric General Circulation Models*. (ed. Eagleson PS), pp. 395–448. Cambridge University Press, Cambridge, UK.

Pielke RA (2001) Influence of the spatial distribution of vegetation and soils on the prediction of cumulus Convective rainfall. *Reviews of Geophysics*, **39**, 151–177.

Pielke RA Sr, Adegoke J, Beltrán-Przekurat A *et al*. (2007) An overview of regional land-use and land-cover impacts on rainfall. *Tellus Series B*, **59**, 587–601.

Pielke RA Sr, Avissar R, Raupach MR, Dolman AJ, Zeng X, Denning AS (1998) Interactions between the atmosphere and terrestrial ecosystems: influence on weather and climate. *Global Change Biology*, **4**, 461–475.

Pielke RA Sr, Marland G, Betts RA *et al*. (2002) The influence of land-use change and landscape dynamics on the climate system: relevance to climate-change policy beyond the radiative effect of greenhouse gases. *Philosophical Transactions of the Royal Society of London. A*, **360**, 1705–1719.

Pielke RA Sr, Pitman A, Niyogi D *et al*. (2011) Land use/land cover changes and climate: modeling analysis and observational evidence. *WIREs Climate Change*, **2**, 828–850.

Pirazzini R (2009) Challenges in snow and ice albedo parameterizations. *Geophysica*, **45**, 41–62.

Pitman AJ, De Noblet-Ducoudré N, Cruz FT *et al*. (2009) Uncertainties in climate responses to past land cover change: first results from the LUCID intercomparison study. *Geophysical Research Letters*, **36**, L14814.

Pongratz J, Reick C, Raddatz T, Claussen M (2008) A reconstruction of global agricultural areas and land cover for the last millennium. *Global Biogeochemical Cycles*, **22**, GB3018.

Qu X, Hall A (2007) What controls the strength of snow-albedo feedback? *Journal of Climate*, **20**, 3971–3981.

Ramankutty N, Foley JA (1999) Estimating historical changes in global land cover: croplands from 1700 to 1992. *Global Biogeochemical Cycles*, **13**, 997–1027.

Ray DK, Welch RM, Lawton RO, Nair US (2006) Dry season clouds and rainfall in northern Central America: implications for the Mesoamerican Biological Corridor. *Global and Planetary Change*, **54**, 150–162.

Ricke KL, Caldeira K (2014) Maximum warming occurs about one decade after a carbon dioxide emission. *Environmental Research Letters*, **9**, 124002.

Roesch A, Roeckner E (2006) Assessment of snow cover and surface albedo in the ECHAM5 general circulation model. *Journal of Climate*, **19**, 3828–3843.

Rogers BM, Randerson JT, Bonan GB (2013) High-latitude cooling associated with landscape changes from North American boreal forest fires. *Biogeosciences*, **10**, 699–718.

Rotenberg E, Yakir D (2010) Contribution of semi-arid forests to the climate system. *Science*, **327**, 451–454.

Rotenberg E, Yakir DaN (2011) Distinct patterns of changes in surface energy budget associated with forestation in the semiarid region. *Global Change Biology*, **17**, 1536–1548.

Rustad L, Campbell J, Marion G *et al*. (2001) A meta-analysis of the response of soil respiration, net nitrogen mineralization, and aboveground plant growth to experimental ecosystem warming. *Oecologia*, **126**, 543–562.

Settele J, Scholes R, Betts S *et al*. (2014) Terrestrial and inland water systems. In: *Climate Change 2014: Impacts,Adaptation, and Vulnerability. Part A: Global and Sectoral Aspects. Contribution of Working Group II to the Fifth Assessment Report of the Intergovernmental Panel on Climate Change* (eds Field CB, Barros VR, Dokken DA, Mach KL, Mastrandrea MD, Bilir TE, Chatterjee M, Ebi KL, Estrada YO, Genova RC, Girma B, Kissel ES, Levy AN, MacCracken S, Mastrandrea PR, White LL), pp. 271–359. Cambridge University Press, Cambridge, UK.

Schwaab J, Bavay M, Davin EL *et al*. (2015) Carbon storage versus albedo change: radiative forcing of forest expansion in temperate mountainous regions of Switzerland. *Biogeosciences*, **12**, 467–487.

Scott CE, Rap A, Spracklen DV *et al*. (2014) The direct and indirect radiative effects of biogenic secondary organic aerosol. *Atmospheric Chemistry and Physics*, **14**, 447–470.

Sellers PJ (1985) Canopy reflectance, photosynthesis, and transpiration. *International Journal of Remote Sensing*, **6**, 1335–1372.

Shell KM, Kiehl JT, Shields CA (2008) Using the radiative kernel technique to calculate climate feedbacks in NCAR's community atmospheric model. *Journal of Climate*, **21**, 2269–2282.

Smith P, Bustamante M, Ahammad H *et al*. (2014) Agriculture, forestry and other land use (AFOLU). In: *Climate Change 2014: Mitigation of Climate Change. Contribution of Working Group III to the Fifth Assessment Report of the Intergovernmental Panel on Climate Change*. (eds Edenhofer O, Pichs-Madruga R, Sokona Y, Farahani E, Kadner S, Seyboth K, Adler A, Baum I, Brunner S, Eickemeier P, Kriemann B, Savolainen J, Schlömer S, von Stechow C, Zwickel T, Minx JC). Cambridge University Press, Cambridge, UK.

Soden BJ, Held IM, Colman R, Shell KM, Kiehl JT, Shields CA (2008) Quantifying climate feedbacks using radiative kernels. *Journal of Climate*, **21**, 3504–3520.

Spracklen DV, Bonn B, Carslaw KS (2008) Boreal forests, aerosols and the impacts on clouds and climate. *Philosophical Transactions of the Royal Society A: Mathematical, Physical and Engineering Sciences*, **366**, 4613–4626.

Stoy PC, Katul GG, Siqueira MBS *et al*. (2006) Separating the effects of climate and vegetation on evapotranspiration along a successional chronosequence in the southeastern US. *Global Change Biology*, **12**, 2115–2135.

Swann ALS, Fung I, Chiang JCH (2011) Mid-latitude afforestation shifts general circulation and tropical precipitation. *PNAS*, **109**, 712–716.

Tetens O (1930) Uber einige meteorologische Begriffe. *z. Geophys*, **6**, 297–309.

Thom AS (1972) Momentum, mass and heat exchange of vegetation. *Quarterly Journal of the Royal Meteorological Society*, **98**, 124–134.

Unger N (2014) Human land-use-driven reduction of forest volatiles cools global climate. *Nature Climate Change*, **4**, 907–910.

Van Vuuren D, Edmonds J, Kainuma M *et al*. (2011) The representative concentration pathways: an overview. *Climatic Change*, **109**, 5–31.

Verseghy DL, Mcfarlane NA, Lazare M (1993) CLASS - A Canadian land surface scheme for GCMs. II. Vegetation model and coupled runs. *International Journal of Climatology*, **13**, 347–370.

Wang K, Dickinson RE (2012) A review of global terrestrial evapotranspiration: observation, modeling, climatology, and climatic variability. *Review of Geophysics*, **50**, RG2005.

Wang Y, Yan X, Wang Z (2014) The biogeophysical effects of extreme afforestation in modeling future climate. *Theoretical and Applied Climatology*, **118**, 511–521.

Wesely ML, Hicks BB (1977) Some factors that affect the deposition rates of sulfur dioxide and similar gases on vegetation. *Journal of the Air Pollution Control Association*, **27**, 1110–1116.

West PC, Narisma GT, Barford CC, Kucharik CJ, Foley JA (2011) An alternative approach for quantifying climate regulations by ecosystems. *Frontiers in Ecology & Environment*, **9**, 126–133.

Winton M (2005) Simple optical models for diagnosing surface-atmosphere shortwave interactions. *Journal of Climate*, **18**, 3796–3806.

Wiscombe WJ, Warren SG (1980) A model for the spectral albedo of snow. I. Pure Snow. *Journal of Atmospheric Science*, **37**, 2712–2733.

Zhang B, Liu Y, Xu D, Cai J, Li F (2011) Evapotranspiration estimation based on scaling up from leaf stomatal conductance to canopy conductance. *Agricultural and Forest Meteorology*, **151**, 1086–1095.

Zhang M, Lee X, Yu G *et al*. (2014) Response of surface air temperature to small-scale land clearing across latitudes. *Environmental Research Letters*, **9**, 034002.

Zhao K, Jackson RB (2014) Biophysical forcings of land-use changes from potential forestry activities in North America. *Ecological Monographs*, **84**, 329–353.

Zheng Y, Yu G, Qian Y, Miao M, Zeng X, Liu H (2002) Simulations of regional climatic effects of vegetation change in China. *Quarterly Journal of the Royal Meteorological Society*, **128**, 2089–2114.